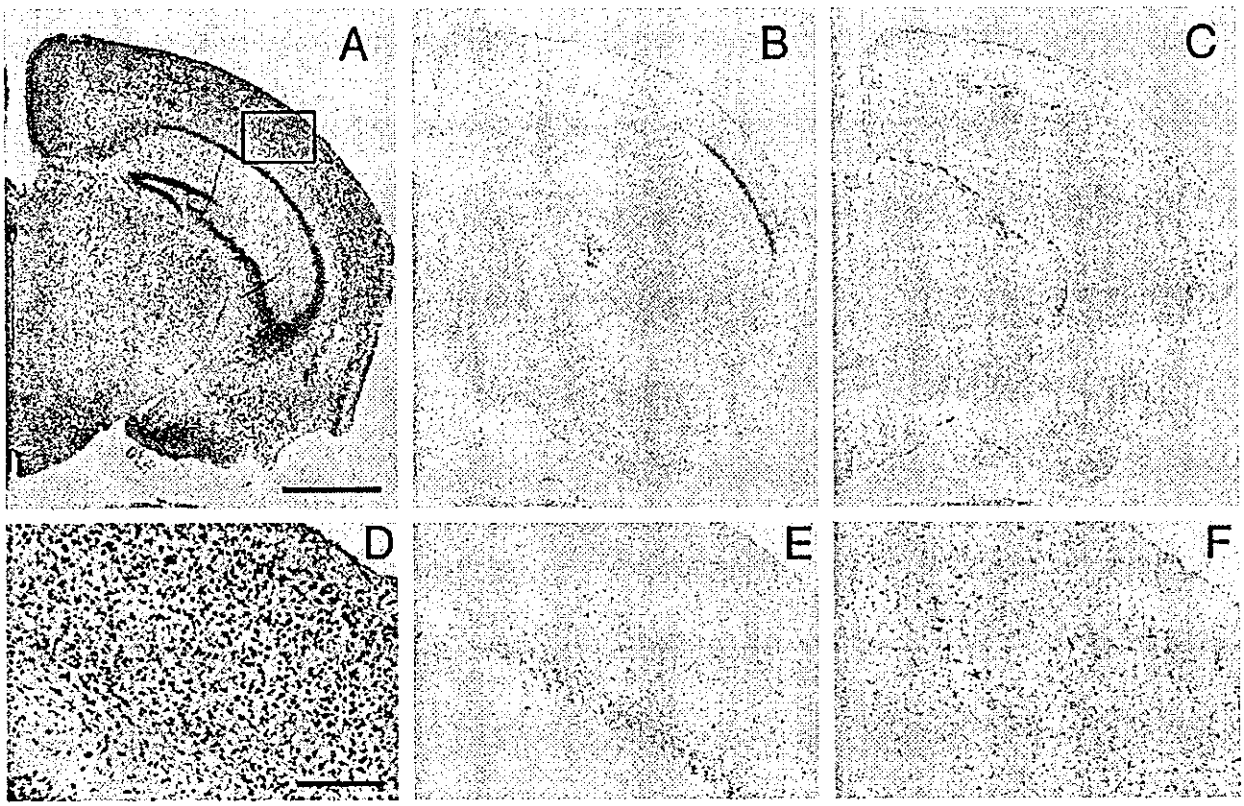

Figure 7. Histological profiles of the mice inoculated with the patient's brain material. A, D: hematoxylin and eosin stain. B, E: prion protein (PrP). C, F: glial fibrillary acidic protein. Spongiform change, PrP deposition and astrocytic gliosis can be observed within the deep layer of the cerebral cortex as well as in the lateral portion of the thalamus. D–F: high power magnifications of the cortical lesions represent the rectangular area depicted in panel A. Bars: 1 mm (A–C), 150 μm (D–E).

pattern of this mouse was distinctive against that of mouse models with other scrapie strains, thus refuting the possibility of contamination. It is not clear whether there were more than two pathogen strains in the brain and whether the strains were dependent on the brain areas. Because we have not examined transmissibility of this case systematically and not obtained frozen materials for Western blot analysis, this aspect still awaits further clarification.

In conclusion, the present case which had FFI genotype showed atypical features, especially with regard to the PrP deposition pattern; there was no deposition within the thalamus or inferior olivary nucleus. Diversity in disease phenotype among patients with the same genotype suggests that some other unidentified factors as well as abnormal PrP deposits or other as yet unknown genetic factors may be responsible for the pathogenesis of the disease. In this study we have shown that variation in pathogen strains may also be one such factor and this factor could have greatly affected the pathogenesis in the present case of FFI.

Acknowledgements

We thank Ms K. Hatanaka for her excellent technical assistance. This study was supported partly by a grant to K. Doh-ura from the Ministry of Health, Labour and Welfare, Japan. Part of this study was carried out at the Morphology Core, Graduate School of Medical Sciences, Kyushu University. The English used in this manuscript was revised by Miss K. Miller (Royal English Language Centre, Fukuoka, Japan).

References

1 Goldfarb LG, Petersen RB, Tabaton M, Brown P, LeBlanc AC, Montagna P, Cortelli P, Julien J, Vital C, Pendelbury WW, Haltia M, Wills PR, Hauw JJ, McKeever PE, Monari L, Schrank B, Swergold GD, Gambetti LA, Gajdusek DC, Lugaresi E, Gambetti P. Fatal familial insomnia and familial Creutzfeldt-Jakob disease: disease phenotype determined by a DNA polymorphism. *Science* 1992; 258: 806–8

2 Manetto V, Medori R, Cortelli P, Montagna P, Tinuper P, Baruzzi A, Rancurel G, Hauw JJ, Vanderhaeghen JJ, Mailleux P, Bugiani O, Tagliavini F, Bouras C, Rizzuto N, Lugaresi E, Gambetti P. Fatal familial insomnia: clinical and pathologic study of five new cases. *Neurology* 1992; 42: 312–9
3 Lugaresi E, Medori R, Montagna P, Baruzzi A, Cortelli P, Lugaresi A, Tinuper P, Zucconi M, Gambetti P. Fatal familial insomnia and dysautonomia with selective degeneration of thalamic nuclei. *N Engl J Med* 1986; 315: 997–1003
4 Parchi P, Petersen RB, Chen SG, Autilio-Gambetti L, Capellari S, Monari L, Cortelli P, Montagna P, Lugaresi E, Gambetti P. Molecular pathology of fatal familial insomnia. *Brain Pathol* 1998; 8: 539–48
5 McLean CA, Storey E, Gardner RJ, Tannenberg AE, Cervenakova L, Brown P. The D178N (cis-129M) 'fatal familial insomnia' mutation associated with diverse clinicopathologic phenotypes in an Australian kindred. *Neurology* 1997; 49: 552–8
6 Zerr I, Giese A, Windl O, Kropp S, Schulz-Schaeffer W, Riedemann C, Skworc K, Bodemer M, Kretzschmar HA, Poser S. Phenotypic variability in fatal familial insomnia (D178N-129M) genotype. *Neurology* 1998; 51: 1398–405
7 Nagayama M, Shinohara Y, Furukawa H, Kitamoto T. Fatal familial insomnia with a mutation at codon 178 of the prion protein gene: first report from Japan. *Neurology* 1996; 47: 1313–6
8 Kawasaki K, Wakabayashi K, Kawakami A, Higuchi M, Kitamoto T, Tsuji S, Takahashi H. Thalamic form of Creutzfeldt-Jakob disease or fatal insomnia? Report of a sporadic case with normal prion protein genotype. *Acta Neuropathol (Berl)* 1997; 93: 317–22
9 Mizusawa H, Ohkoshi N, Sasaki H, Kanazawa I, Nakanishi T. Degeneration of the thalamus and inferior olives associated with spongiform encephalopathy of the cerebral cortex. *Clin Neuropathol* 1988; 7: 81–6
10 Taniwaki Y, Hara H, Doh-Ura K, Murakami I, Tashiro H, Yamasaki T, Shigeto H, Arakawa K, Araki E, Yamada T, Iwaki T, Kira J. Familial Creutzfeldt-Jakob disease with D178N-129M mutation of PRNP presenting as cerebellar ataxia without insomnia. *J Neurol Neurosurg Psychiatry* 2000; 68: 388
11 Sasaki K, Doh-ura K, Ironside JW, Iwaki T. Increased clusterin (apolipoprotein J) expression in human and mouse brains infected with transmissible spongiform encephalopathies. *Acta Neuropathol (Berl)* 2002; 103: 199–208
12 Safar J, Wille H, Itri V, Groth D, Serban H, Torchia M, Cohen FE, Prusiner SB. Eight prion strains have PrP (Sc) molecules with different conformations. *Nat Med* 1998; 4: 1157–65
13 Tateishi J, Brown P, Kitamoto T, Hoque ZM, Roos R, Wollman R, Cervenakova L, Gajdusek DC. First experimental transmission of fatal familial insomnia. *Nature* 1995; 376: 434–5
14 Parchi P, Capellari S, Gambetti P. Intracerebral distribution of the abnormal isoform of the prion protein in sporadic Creutzfeldt-Jakob disease and fatal insomnia. *Microsc Res Tech* 2000; 50: 16–25
15 Almer G, Hainfellner JA, Brucke T, Jellinger K, Kleinert R, Bayer G, Windl O, Kretzschmar HA, Hill A, Sidle K, Collinge J, Budka H. Fatal familial insomnia: a new Austrian family. *Brain* 1999; 122: 5–16
16 Sherriff FE, Bridges LR, Gentleman SM, Sivaloganathan S, Wilson S. Markers of axonal injury in post mortem human brain. *Acta Neuropathol (Berl)* 1994; 88: 433–9
17 Ferrer I, Puig B, Blanco R, Marti E. Prion protein deposition and abnormal synaptic protein expression in the cerebellum in Creutzfeldt-Jakob disease. *Neuroscience* 2000; 97: 715–26
18 Liberski PP, Budka H. Neuroaxonal pathology in Creutzfeldt-Jakob disease. *Acta Neuropathol (Berl)* 1999; 97: 329–34
19 Montagna P, Gambetti P, Cortelli P, Lugaresi E. Familial and sporadic fatal insomnia. *Lancet Neurol* 2003; 2: 167–76

Received 4 February 2004
Accepted after revision 26 April 2004

Diffusion-weighted MRI abnormalities as an early diagnostic marker for Creutzfeldt–Jakob disease

Y. Shiga, MD, PhD; K. Miyazawa, MD; S. Sato, MD, PhD; R. Fukushima, MD; S. Shibuya, MD, PhD; Y. Sato, MD, PhD; H. Konno, MD, PhD; K. Doh-ura, MD, PhD; S. Mugikura, MD, PhD; H. Tamura, MD, PhD; S. Higano, MD, PhD; S. Takahashi, MD, PhD; and Y. Itoyama, MD, PhD

Abstract—*Objective:* To evaluate the usefulness of diffusion-weighted MRI (DWI) for the early diagnosis of Creutzfeldt–Jakob disease (CJD). *Methods:* Thirty-six consecutive patients (age 56 to 82 years) were enrolled, and 26 were examined by DWI. Nine were definite based on the World Health Organization criteria, and 27 were probable. The percentages of DWI abnormalities, periodic sharp wave complexes (PSWCs) on the EEG, detection of CSF 14-3-3 protein, and increase of CSF neuron-specific enolase (>25 ng/mL) on the first examination were compared. For DWI, 32 patients (age 31 to 84 years) who showed progressive dementia or impaired consciousness served as disease controls. *Results:* The percentage of DWI abnormalities was 92.3%, of PSWCs 50.0%, of 14-3-3 protein detection 84.0%, and of NSE increase 73.3%. Two of the 32 control subjects were falsely positive on DWI. The sensitivity of DWI was 92.3% (95% CI 74.8 to 99.5%) and specificity 93.8% (95% CI 79.2 to 99.2%). In 17 patients who did not show PSWCs on the first EEG, abnormal DWI findings were still clearly detected. Four patients who were negative for 14-3-3 protein also showed DWI abnormalities. DWI abnormalities were detected as early as at 3 weeks of symptom duration in four patients in whom PSWCs were not yet evident. *Conclusions:* DWI can detect characteristic lesions in the majority of patients with CJD regardless of the presence of PSWCs. DWI was the most sensitive test for the early clinical diagnosis of CJD; consideration should be given to its inclusion in the clinical diagnostic criteria of CJD.

NEUROLOGY 2004;63:443–449

Creutzfeldt–Jakob disease (CJD) is a transmissible, progressive, fatal spongiform encephalopathy.[1] The transmission of bovine spongiform encephalopathy to humans as variant CJD[2] has focused increased attention on CJD. The cardinal manifestations of the disease are rapidly progressive dementia, generalized myoclonus, and periodic sharp wave complexes (PSWCs) on EEG. However, cases that do not consistently show such typical manifestations have been recognized, and the spectrum of disease manifestations has been extending.[3,4] An early and accurate diagnosis is important to prevent disease transmission, but diagnosis is not easy, especially in the early stage of the disease.

PSWCs on EEG have been used as one of the central diagnostic tests for CJD.[5] However, PSWCs are observed in only 60% of patients[3,4] and usually appear after the middle stage of the disease. In addition, PSWCs are not always specific for CJD.[6] PSWCs are therefore of limited use for the early diagnosis of CJD. The detection of brain-specific proteins such as 14-3-3 protein[6] and neuron-specific enolase[7] (NSE) in CSF also supports the diagnosis of CJD. Although the sensitivity and specificity of 14-3-3 protein[6] and NSE[7] are higher than those of PSWCs,[8] false-positive results are observed in several neurologic diseases such as herpes simplex encephalitis, cerebrovascular disease,[6] Hashimoto encephalopathy,[9] and paraneoplastic neurologic disorders.[10]

Recently, several reports described that diffusion-weighted MRI (DWI) could demonstrate early brain lesions in CJD patients when scans were negative on T2-weighted MRI examination (T2I).[11] In this study, we evaluated the usefulness of DWI for the early clinical diagnosis of CJD by comparing it with other MR sequences such as T2I and fluid-attenuated inversion recovery imaging (FLAIR) and with other diagnos-

See also pages 410, 436, and 450

From the Department of Neurology (Drs. Shiga, Miyazawa, and Itoyama), Tohoku University School of Medicine, Department of Neurology (Dr. S. Sato), Kohnan Hospital, Second Department of Internal Medicine (Dr. Fukushima), Hiraka General Hospital, Department of Neurology (Dr. Shibuya), Miyagi National Hospital, Department of Neurology (Dr. Y. Sato), Research Institute for Brain and Blood Vessels, Akita, Department of Neurology (Dr. Konno), Nishitaga National Hospital, Department of Neuropathology (Dr. Doh-ura), Institute of Brain Diseases, Kyushu University Faculty of Medicine, and Department of Diagnostic Radiology (Drs. Mugikura, Tamura, Higano, and Takahashi), Tohoku University School of Medicine, Japan.

Presented in part at the 127th Annual Meeting of the American Neurologic Association, October 14, 2002, New York.

Received April 16, 2003. Accepted in final form March 18, 2004.

Address correspondence and reprint requests to Dr. Y. Shiga, Department of Neurology, Tohoku University School of Medicine, 1-1 Seiryo-machi, Aoba-ku, Sendai 980-8574, Japan; e-mail: yshiga@em.neurol.med.tohoku.ac.jp

Table 1 Profiles of CJD patients and examination results

Patient no.	Type	Age/sex	Duration, wk	DL	*PRNP*	PSWC	DWI	14-3-3	NSE, ng/mL
1	Sp	71/M	3	P	MM	−/+	+		
2	Sp	63/M	4	P	MM	+	+		26
3	Sp	78/M	6	P	MM	+	+	+	79
4	Sp	76/F	6	P	MM	+	+	−	22
5	Sp	61/M	7	P	MM	+	+	+	37.3
6	Sp	66/M	8	P	MM	−/+	+	+	29
7	Sp	76/F	8	P	MM	+	+	+	177
8	Sp	69/M	8	P	MM	+			
9	Sp	54/M	8	P	MM	−/+	+	+	18.4
10	Sp	69/M	8	D	VV2	−	+	+	110
11	Sp	68/M	9	P	MM	−/+	+	+	24
12	Sp	63/F	9	P	MM	+		+	56
13	Sp	74/M	10	D	MM	+			31
14	Sp	71/M	12	P	MM	+		+	25.2
15	Sp	63/F	12	P	MM	−/+	+	+	
16	Sp	79/M	13	D	MM	+		+	36
17	Sp	75/F	21	D	VV2	−	+	+	48
18	Sp	74/F	23	P	MM	+	+	+	51.4
19	Sp	59/M	24	D	MM2-T	−	−	−	15.4
20	Sp	73/F	25	P	MV	−	+	+	56.2
21	Sp	73/F	3	P		−/+	+		
22	Sp	69/M	3	P		−/+	+		50
23	Sp	67/F	6	P		+		+	95
24	Sp	70/M	8	P		+	−/+		
25	Sp	72/F	8	P		+			120
26	Sp	59/M	9	P		+	+		62
27	Sp	74/F	17	D		+		+	72
28	Sp	66/F	25	P		+		+	300
29	Fa	76/M	4	P	V180I	−	+	+	19.5
30	Fa	56/F	8	P	M232R	−/+	+	+	110
31	Fa	58/M	9	P	E200K	−/+	+		
32	Fa	72/M	12	D	V180I	−	+		60.4
33	Fa	82/F	13	P	V180I	−	+	+	32.1
34	Fa	79/M	24	D	V180I	−	+	−	13
35	Ia (Dura)	57/M	3	D	MM	−/+	+	−	18
36	Ia (Dura)	70/F	8	P		+		+	15.8

CJD = Creutzfeldt–Jakob disease; Duration, wk = duration from the onset to diagnostic examinations; DL = diagnostic level based on World Health Organization criteria; PSWC = periodic sharp wave complex; DWI = diffusion-weighted imaging; NSE = neuron-specific enolase; Sp = sporadic CJD; P = probable; MM = homozygosity for methionine at codon 129; D = definite; VV = homozygosity for valine at codon 129; MV = methionine/valine heterozygosity at codon 129; Fa = familial CJD; V180I = a point mutation of Val to Ile at codon 180; M232R = a point mutation of Met to Arg at codon 232; E200K = a point mutation of Glu to Lys at codon 200; Ia = iatrogenic CJD; Dura = a recipient of cadaveric dura mater; (−/+) = negative on the first examination but positive on the sequential examinations.

tic tests including PSWC, CSF 14-3-3 protein, and CSF NSE, which are used as the World Health Organization (WHO) CJD diagnostic criteria.[12]

Patients and methods. *Study group.* Thirty-six consecutive patients with CJD seen from January 1, 1994, to June 30, 2003, at the Department of Neurology, Tohoku University Hospital, and its related hospitals (age 56 to 82 years with a mean age of 68.9 years; 21 men) were enrolled in this study. These patients included the patients in our previous reports.[13-15] According to the WHO criteria,[12] 9 were definite and 27 were probable. A genetic study of human prion protein gene (*PRNP*) was performed in 27 patients, and 20 were sporadic CJD (17 had methionine homozygosity at codon 129 of *PRNP*, and, among those, 3 were definite; 14 were probable at the diagnostic level, and 2 who were definite had valine homozygosity and 1 who was probable had methionine/valine heterozygosity). Six had familial CJD (two definite, four probable, in which two had V180I[15] and one had E200K[16]; one had M232R).[17] Of two patients who were recipients of cadaveric dura mater (iatrogenic CJD), one was definite and one was probable (one had methionine homozygosity at codon 129 of *PRNP*). Our patients composed various clinical phenotypes of CJD including uncommon variants with rather longer clinical courses. The profiles of these patients are listed in table 1.

Disease control group. We reviewed retrospectively the clinical records of our patients who were admitted to the Department of Neurology, Tohoku University Hospital, from January 1, 1998, to June 30, 2003. Excluding patients who had an abrupt onset or symptoms suggesting meningoencephalitis, such as high fever, stiff neck, etc., 81 patients demonstrated subacute dementia or impaired consciousness progressing for 1 to several months.

Table 2 Final diagnosis of control patients

Final diagnosis	Total no.
Metabolic encephalopathy, including one alcoholic encephalopathy	4
Dementia with Lewy bodies	3
Corticobasal ganglionic degeneration	3
Cerebrovascular dementia	2
Viral encephalitis, including one herpes simplex encephalitis	3
Interval form of CO poisoning	3
Cryptococcal meningoencephalitis	2
Mitochondrial cytopathy	2
Progressive dementia, not otherwise specified	4
Alzheimer disease	1
CNS lymphoma	1
Multiple sclerosis	1
Temporal lobe epilepsy	1
Leukoencephalopathy, not otherwise specified	1
Ganser syndrome	1
Total	32

Thirty-two (age 31 to 84 years with a mean age of 61.9 years; 15 men) of 81 patients had undergone DWI examination. They served as disease controls for DWI because obtaining a large group of individuals with suspected CJD but with an alternative diagnosis was difficult. Of these patients, four had seriously suspected CJD, for whom the final diagnosis in two was metabolic encephalopathy that was improved by IV vitamin administration, one was mitochondrial encephalopathy as confirmed by an enzyme assay, and one was corticobasal ganglionic degeneration verified by autopsy. These controls included dementia with Lewy bodies, Alzheimer disease (AD), cerebrovascular disease, CNS infection, metabolic or mitochondrial encephalopathy, CNS malignancy, corticobasal ganglionic degeneration, interval form of CO intoxication, etc. Dementia with Lewy bodies, AD, and cerebrovascular disease are major differential diagnoses of CJD,[18] and CNS infection, encephalopathy, and CNS malignancy sometimes demonstrate positive 14-3-3 protein test in CSF,[19] which is an important diagnostic marker for CJD.[6] The disease controls are listed in table 2.

We compared the sensitivities of the positive results of MR sequences such as DWI, T2I, and FLAIR. We also assessed interobserver agreement. We compared the sensitivities of the positive results of DWI, PSWC, and brain-specific proteins such as 14-3-3 protein and NSE in CSF for making a diagnosis of CJD. PSWC and positive assay of 14-3-3 protein are included in the WHO diagnostic criteria.[12] These examinations were carried out 3 to 25 weeks after the onset with a mean duration of 10.7 weeks after the onset (see table 1).

Methods. DWI technique. Scans were performed on a number of units. A 1.5 or 1.0 T MR unit (Signa Horizon LX, GE Medical Systems, Milwaukee, WI; or Magnetom Vision, Siemens, Erlangen, Germany) was used. DWI was performed in 26 CJD cases with single-shot spin-echo echo-planar imaging. Imaging parameters were as follows: 4,700 to 5,000/93 to 120/1 or 2 (repetition time/effective echo time/no. excitations), 10 to 15 axial sections of 5- or 6-mm section thickness with a 1.5- to 3.0-mm intersection gap, 128 × 128 matrix, 220- or 230-mm field of view, and a diffusion-encoding strength (*b* factor) of 1,000 s/mm^2. In 23 of 26 CJD cases, T2I was performed, and in 17 of 26 CJD cases, FLAIR was performed. DWI, T2I, and FLAIR were performed on the same day using the same MR unit.

MRI investigation. MRI scans were assessed retrospectively as hard copies by two well-experienced neuroradiologists blind to clinical information, who examined each type of sequence separately, without referring to the other MR sequences, independently and individually. We accepted three types of high-intensity lesions as CJD-related lesions on DWI: lesions in the striatum (caudate or putaminal or both), lesions in the thalamus including the pulvinar, and lesions along the cortical ribbon (cerebral or cerebellar). We also accepted the lesions of several types in combination. We accepted not only the symmetric lesions but also asymmetric or unilateral lesions. DWI scans of the disease control group were also assessed retrospectively as hard copies combined with five DWI scans of CJD patients by the same two neuroradiologists, completely blind to clinical information to minimize observer bias.

PSWCs. EEG was recorded using the International 10–20 System. PSWCs were defined as diffuse biphasic or triphasic sharp wave complexes with a duration between 100 and 600 milliseconds and an intercomplex interval between 500 and 2,000 milliseconds.[5]

Brain-specific proteins in CSF. 14-3-3 protein immunoassay in CSF by means of western blotting was performed using a polyclonal antibody to the β isoform of 14-3-3 protein, SC 629 (Santa Cruz Biotechnology, Santa Cruz, CA). The presence of the band against the antibody, SC 629, was investigated. NSE in CSF was measured commercially using an ELISA (SRL Laboratory, Tokyo, Japan), and a value of >25 ng/mL[20] was judged as positive.

Statistical analyses of the diagnostic sensitivities of DWI, PSWCs, and NSE and 14-3-3 protein in CSF, positive rate of DWI, T2I, and FLAIR, and interobserver agreement rate were done using the Fisher exact probability test.

Results. *MRI.* DWI was examined in 26 CJD patients 3 to 25 weeks after the onset with a mean duration of 10.7 weeks. Twenty-four CJD patients showed high-intensity brain lesions by DWI examination. For both observers, the sensitivity of DWI for the CJD diagnosis was 92.3%. The interobserver agreement rate was 100%. Three patients (12.5%) showed lesions only in the caudate heads and putamen, 10 (41.7%) patients showed linear lesions only in the cerebral cortex, and 11 (45.8%) patients showed lesions in both the basal ganglia and the cerebral cortex (figure 1). Among them, only three patients (12.5%) showed lesions in the thalamus. No patients showed high-intensity lesions in the cerebellum. High-intensity lesions on DWI appeared before brain atrophy. The lesions involving the striatum were not always symmetric at the beginning but later became symmetric (figure 2), although symmetric striatal lesions are well known in CJD.[11] In some cases, the high-intensity lesions with sequential DWI did not always progress with the advance of the disease, and the signal intensity sometimes decreased with the disease progression in some lesions. In some cases, the cortical high signal varied in intensity and anatomic distribution (figure 3). In the terminal stage with profound brain atrophy, the high-intensity lesions became unclear. T2I was examined in 23 of 26 DWI-examined patients, but one T2I scan was excluded because of the low quality due to motion artifacts. One observer judged that 11 of 22 patients were positive (50.0%), and another observer judged that 8 were positive (36.4%). The interobserver agreement rate was 68.2%, and it was lower than that of DWI ($p < 0.005$). In both observers, DWI was more sensitive than T2I ($p < 0.005$ for one observer and $p < 0.0005$ for another observer). FLAIR was examined in 17 of 26 patients. One observer judged that 10 of 17 patients were positive (58.8%), and another observer judged that 7 were positive (41.2%). The interobserver agreement rate was 82.4%, and this also was lower than that of DWI ($p < 0.05$). DWI was more sensitive than FLAIR ($p < 0.01$ for one observer and $p < 0.0005$ for another observer). We show in figure 4 an example in which only DWI could detect abnormal high-intensity lesions.

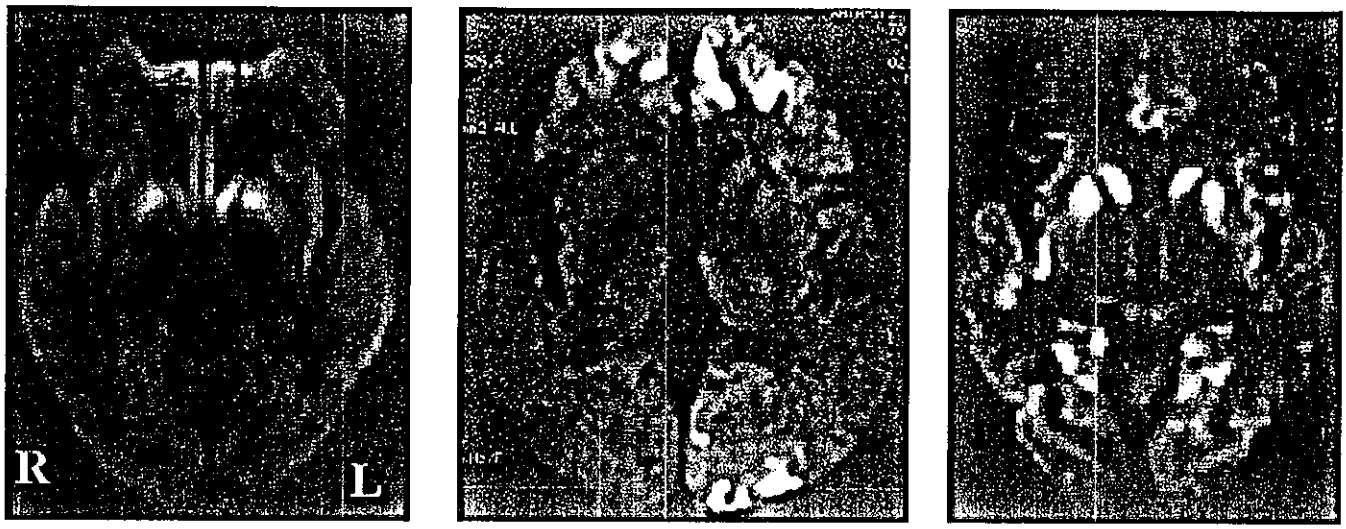

Figure 1. MRI changes seen in Creutzfeldt–Jakob disease. Three patterns of high-intensity lesions were seen: striatal lesion (A), cerebral cortical lesion (B), and a combination of both lesions (C).

DWI failed to detect any lesions in two patients at the first examination. The second DWI showed high-intensity lesions at the striatum in one of those patients. Repeated DWI scans of the other patient did not show any high-intensity lesions throughout his disease course. On the postmortem examination, protease-resistant type 2 prion protein was detected in this patient by western blot analysis using monoclonal antibody 3F4 (Signet Laboratories, Dedham, MA), and there were no spongiform changes. This case was classified as MM2-thalamic according to Parchi's classification (table 1).[3]

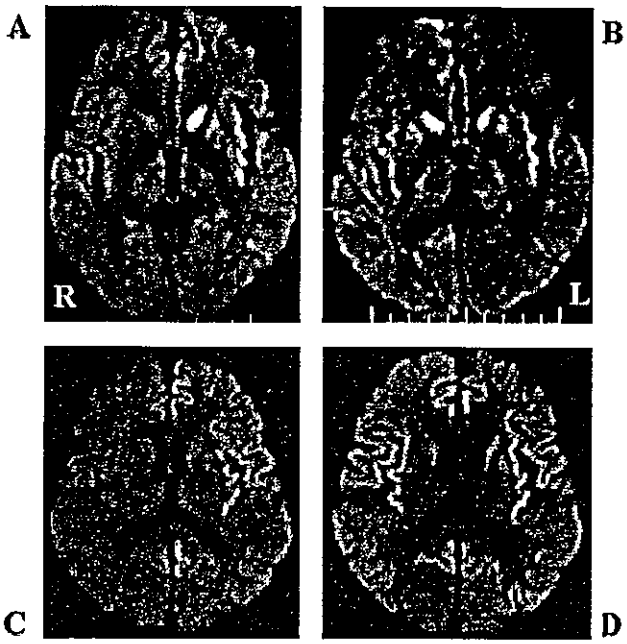

Figure 2. Chronologic change of the striatal and cortical lesions. A case of sporadic Creutzfeldt–Jakob disease (CJD) showing the progression of the basal ganglia signal changes from asymmetric (A) to symmetric (B). The interval between (A) and (B) was 2 months. A case of familial CJD with V180I mutation showing the progression of the cerebral cortex and caudate head signal changes from asymmetric (C) to symmetric (D). The interval between (C) and (D) was 4 months.

High-intensity DWI lesions that were in agreement with our criteria were observed in the disease control patients. One observer judged that a 69-year-old woman with cryptococcal meningoencephalitis and a 60-year-old woman with interval form of CO poisoning were falsely positive. Another observer judged that a 48-year-old woman with herpes simplex encephalitis and a 47-year-old with alcoholic encephalopathy were falsely positive. For both observers, the false-positive rate was 6.3% and the interobserver agreement rate was 87.5%. No highly CJD-suspected patients demonstrated high-intensity lesions. The sensitivity of DWI was 92.3% (95% CI 74.8 to 99.5%) and specificity 93.8% (95% CI 79.2 to 99.2%).

DWI detected the brain lesions before the appearance of PSWCs on EEG in 10 patients. DWI abnormalities were detected as early as at 3 weeks of symptom duration in four patients in whom PSWCs were not yet evident. In seven of eight patients who did not show PSWCs throughout their disease course, the first DWI clearly demonstrated the brain lesions (see table 1).

PSWCs on EEG. EEG was recorded from all 36 patients. Eighteen of 36 (50.0%) patients showed PSWCs that fit the criteria on the first EEG. In 10 of 18 PSWC-negative patients, sequential EEG showed PSWCs. However, eight patients (22.2%) did not show PSWCs in further sequential EEG recordings. The genetic analysis of *PRNP* demonstrated that four had a point mutation of V180I and one had MV at codon 129, and the postmortem examination revealed that two had VV2 and one had MM2-thalamic (see table 1). Generally, these types of CJD patients do not show PSWCs.[3]

Brain-specific proteins in CSF. The 14-3-3 protein was examined in 25 patients and NSE in 30. Twenty-one of those 25 patients (84.0%) were positive for 14-3-3 protein

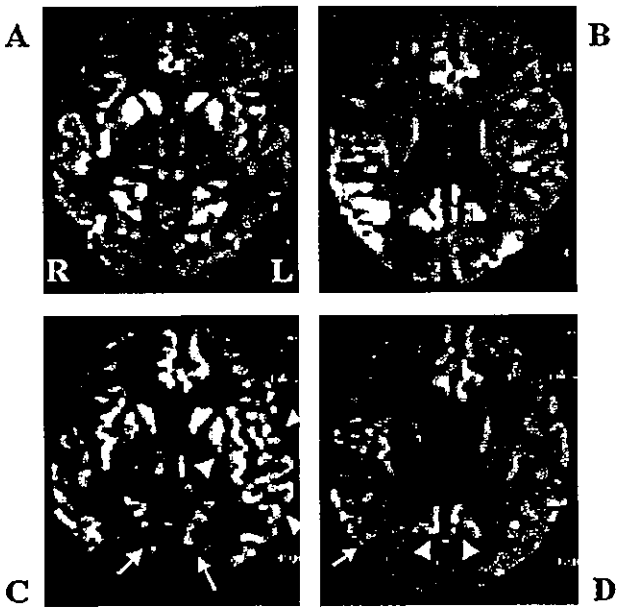

Figure 3. Chronologic change of the cortical lesions in sporadic Creutzfeldt–Jakob disease (sCJD). The cortical high intensity seen in a case of sCJD changed with time, with both increases and decreases in signal intensity in different areas. The high intensity in the bilateral occipital cortices (A) decreased (C, arrows), whereas the signal intensity in the left insular and temporal cortices (A) apparently increased (C, arrowheads). The interval between (A) and (C) was 1 month. The high intensity in the right temporal cortex and bilateral occipital cortices (B) decreased (D, arrow for the left temporal cortex and arrowheads for the bilateral medial occipital cortices). The interval between (B) and (D) was 1 month. Note that the high-intensity lesions depicted in diffusion-weighted imaging did not simply expand with the advance of the disease.

and 22 of those 30 patients (73.3%) were positive for NSE. In 24 patients examined for both brain-specific proteins, 16 were positive for both, 4 were negative for both, and 4 NSE-negative patients were positive for 14-3-3 protein (see table 1).

Comparison of sensitivity of DWI, PSWCs on EEG, and brain-specific CSF protein assay in diagnosing CJD. The sensitivity of DWI examined for the differential diagnosis was 92.3%, of PSWCs 50.0%, of 14-3-3 protein 84.0%, and of NSE 73.3%. DWI was more sensitive than PSWCs ($p < 0.0005$). 14-3-3 protein was more sensitive than PSWCs ($p < 0.01$). DWI tended to be more sensitive than 14-3-3 protein and NSE, but the differences were not significant ($p = 0.36$ and $p = 0.06$) (figure 5). In all 10 patients who had PSWCs in the sequential EEG recording, the lesions had already been detected earlier by DWI. DWI was positive in three of four 14-3-3 protein-negative patients and in six of seven NSE-negative patients. In only one patient who was classified as a rare variant of MM2-thalamic,[3] DWI, PSWC, 14-3-3 protein, and NSE were all negative.

Discussion. MRI had not been thought to be a sensitive noninvasive diagnostic test of CJD[21]; it was previously thought that EEG was the most reliable diagnostic test.[5] Increased signal intensity in the basal ganglia on T2I was first described in 1988,[22] and it was demonstrated that MRI was useful in depicting the lesions of CJD.[23] Although the usefulness of DWI for the early diagnosis of CJD has been suggested,[11,13] no one has compared the ability to depict the lesions among MR sequences such as T2I, FLAIR, and DWI or the accuracy of DWI in diagnosing CJD, especially for the early clinical diagnosis of CJD, with other noninvasive tests including EEG. In this study, we found that the sensitivity of DWI was 92.3% and that DWI was significantly more sensitive than conventional T2I and FLAIR in detecting the CJD-related lesions. T2I and FLAIR, whose sensitivities were 40 to 50%, are inadequate as a test for the first-line differential diagnosis. Further, the CJD-related lesions that we demonstrated on DWI were not detected in a small number of controls with AD, dementia with Lewy bodies, and cerebrovascular dementia, which are the major differential diagnoses of CJD.[18] We have demonstrated the superiority of DWI over the other noninvasive diagnostic tests by comparing its sensitivity with that of PSWCs on EEG, 14-3-3 protein, and NSE examined for the differential diagnosis. Unexpectedly, the interobserver agreement rate of DWI was 100%, and it was significantly higher than that of T2I and FLAIR. This indicates that DWI, which can depict the CJD-related lesions clearly and reliably, may represent a very important diagnostic test for the differential diagnosis. As we demonstrated previously,[13] DWI is more tolerant of motion artifacts than T2I and FLAIR. This advantage is especially important in CJD patients with the involuntary movement of myoclonic jerk. This tolerance may be one of the reasons for the higher sensitivity and the higher interobserver agreement rate of DWI compared with T2I and FLAIR.

The positive rates of T2I by our two observers were 36.4 and 50.0%, and these were significantly lower than a previously reported positive rate for T2I of 79.3%.[23] We think that this discrepancy can be accounted for by the difference in the time when the MRI was examined; the mean duration for our patients from the onset to MRI examination was 10.7 weeks (2.6 months), whereas that of the previous report was 8.1 months.[23] A positive rate for T2I of 67.3% was also reported; however, the positive rate of the first T2I in that report was 43.2%.[24] This is almost the same as in our results.

Currently, PSWCs play a central role in the diagnosis of CJD.[12] However, in the case of PSWC-negative patients, the diagnosis of CJD is sometimes difficult, and such cases are classified as "possible CJD."[12] We have demonstrated in this study not only that DWI was positive earlier than the presence of PSWCs but also that DWI was positive in CJD subjects without PSWCs throughout their disease. In the suspected CJD patients who are diagnosed as "possible CJD," the accuracy of the diagnosis is different between DWI-positive patients and DWI-negative patients. The likelihood of CJD is higher in

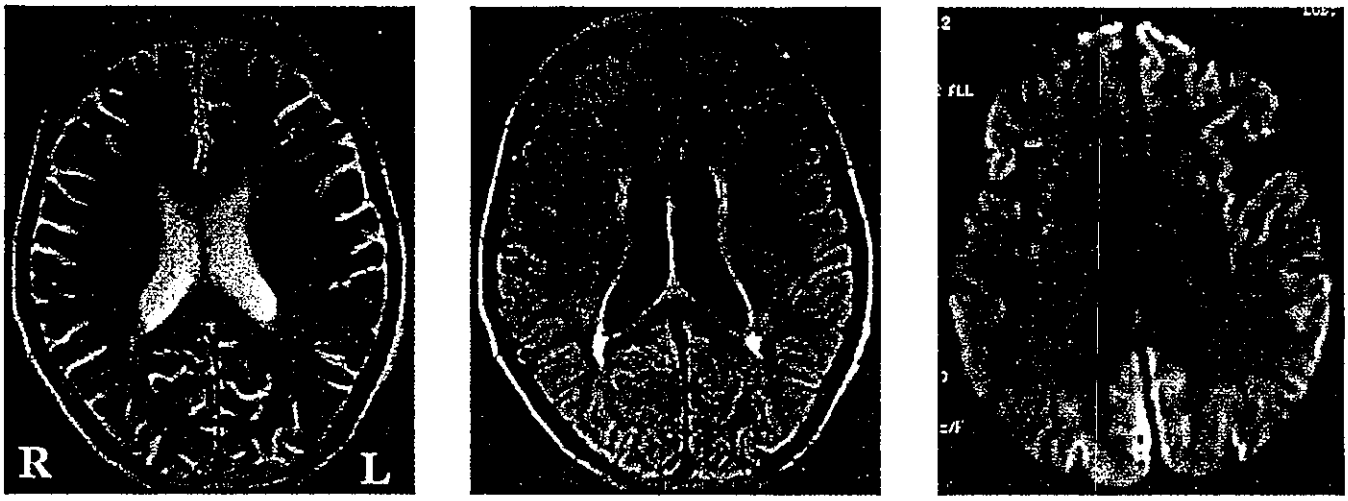

Figure 4. Comparison of conspicuity of Creutzfeldt–Jakob disease–related changes of the same patient on different MRI sequences. T2-weighted imaging (A) and fluid-attenuated inversion recovery imaging (B) show normal findings, and diffusion-weighted MRI (C) demonstrates high-intensity lesions in the cerebral cortex.

DWI-positive patients and lower in DWI-negative patients.

Each observer judged as false positive 2 of 32 disease controls. However, two observers did not agree on the result: one observer judged DWI of cryptococcal meningoencephalitis and interval form of CO poisoning as false positive, and another observer judged DWI of herpes simplex encephalitis and alcoholic encephalopathy as false positive. However, a careful history taking and the presence of pleocytosis in the CSF study significantly reduced the possibility of CJD. DWI was very useful to distinguish CJD from AD, vascular dementia, and dementia with Lewy bodies, which are the major differential diagnoses of CJD[18] and account for the vast majority of dementia in elderly patients.[25] DWI of mitochondrial encephalopathy, lactic acidosis, and stroke-like episodes (MELAS), Wilson disease, and Wernicke encephalopathy can demonstrate similar abnormalities. However, the clinical course and laboratory findings easily distinguish them from CJD. DWI in hypoglycemia,[26] anoxia,[27] and reversible posterior leukoencephalopathy syndrome[28] has also been reported to demonstrate high-intensity lesions similar to those of CJD. However, these have peculiar episodes, and the onset is apparently different from that of CJD. We must mention a 15-year-old boy with a final diagnosis of CNS lupus who was referred to the Japanese CJD Surveillance Committee. His consciousness disturbance developed subacutely, and his DWI showed scattered high-intensity lesions in the cerebral cortex and basal ganglia. His neurologic symptoms improved after the administration of prednisolone. CNS vasculitic disease also needs to be excluded in the differential diagnosis.

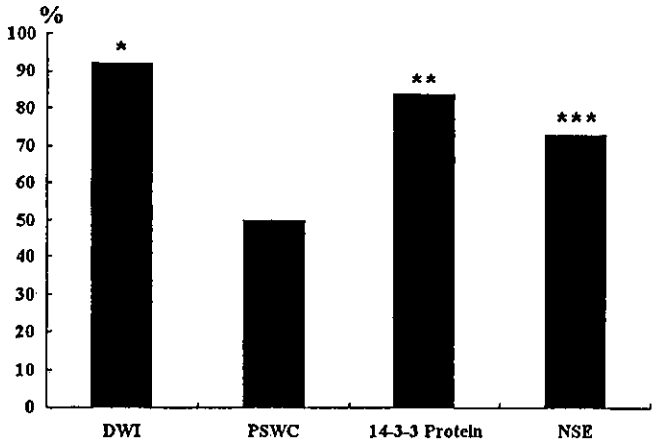

*Figure 5. Percentage of Creutzfeldt–Jakob disease cases with positive test. The positive rates of diffusion-weighted MRI (DWI), periodic sharp wave complexes (PSWCs), 14-3-3 protein, and neuron-specific enolase (NSE) examined for the differential diagnosis were 92.3, 50.0, 84.0, and 73.3%. *DWI was more sensitive than PSWCs ($p < 0.0005$). **14-3-3 protein was more sensitive than PSWCs ($p < 0.01$). *DWI tended to be more sensitive than 14-3-3 protein ($p = 0.36$) and NSE ($p = 0.06$). ***NSE tended to be more sensitive than PSWCs ($p = 0.053$). However, these were not significant.*

The kinds of pathologic findings that correlate with the CJD-related high-intensity lesions demonstrated in DWI are still controversial. Spongiform changes[29] and prion protein deposits[30] are candidates. The time lag from DWI examination to postmortem pathologic examination impedes an accurate understanding. The postmortem examination in one case of familial CJD with V180I whose DWI showed prominent high intensity in the cerebral cortex revealed severe spongiform changes and rather weak prion protein staining there immunohistochemically. The postmortem examination in a patient with spo-

radic CJD with MM2-thalamic whose DWI demonstrated negative findings throughout the disease course revealed no spongiform changes and rather weak prion protein staining. Based on our limited experience, we speculate that the high-intensity lesions depicted by DWI are related to spongiform changes rather than to prion protein deposition; however, more animal and postmortem studies are required to confirm this. It remains unclear why some high-intensity lesions become less prominent with the advance of the disease. We need to accumulate radiopathologic studies for several types of CJD.

The weaknesses of this study are that the number of ideal controls, CJD suspects with a final alternative diagnosis, was too small, because it was difficult to obtain a large number of such patients, and also the lack of pathologic diagnosis in the majority of CJD patients, with the result that only 9 of 36 patients were definite because of the difficulty in obtaining a postmortem examination in many cases. To overcome these weak points, a multicenter analysis of pathologically verified CJD patients and ideal controls is needed.

Last, in interpreting the results of the diagnostic tests, we must understand that such laboratory tests as DWI, brain-specific protein, and EEG reflect different aspects of the disease. Brain-specific proteins reflect the ongoing rapid and massive destruction of the neurons, and EEG reflects the current state of the injured brain.

Acknowledgment

The authors thank Drs. Keiji Chida, Nobuyuki Sato, Reiko Fukatsu, Takanori Oikawa, Hiroshi Kuroda, Takafumi Hasegawa, Atsushi Takeda, Akio Kikuchi, Naoki Suzuki, Masahiro Asano, and Kazutaka Jin for the patients' care. They also thank Dr. Tetsuyuki Kitamoto for analyzing the prion protein gene and Mr. Brent Bell for reading the manuscript.

References

1. Masters CL, Harris JO, Gadujeck DC, et al. Creutzfeldt–Jakob disease: patterns of worldwide occurrence and the significance of familial and sporadic clustering. Ann Neurol 1979;5:177–188.
2. Will RG, Ironside JW, Zeidler M, et al. A new variant of Creutzfeldt–Jakob disease in the UK. Lancet 1996;347:921–925.
3. Parchi P, Giese A, Capellari S, et al. Classification of sporadic Creutzfeldt–Jakob disease based on molecular and phenotypic analysis of 300 subjects. Ann Neurol 1999;46:224–233.
4. Zerr I, Schulz-Schaeffer WJ, Giese A, et al. Current clinical diagnosis in Creutzfeldt–Jakob disease: Identification of uncommon variants. Ann Neurol 2000;48:323–329.
5. Steinhoff BJ, Räcker S, Herrendorf G, et al. Accuracy and reliability of periodic sharp wave complexes in Creutzfeldt–Jakob disease. Arch Neurol 1996;53:162–166.
6. Zerr I, Bodemer M, Gefeller O, et al. Detection of 14-3-3 protein in the cerebrospinal fluid supports the diagnosis of Creutzfeldt–Jakob disease. Ann Neurol 1998;43:32–40.
7. Zerr I, Bodemer M, Räcker S, et al. Cerebrospinal fluid concentration of neuron-specific enolase in diagnosis of Creutzfeldt–Jakob disease. Lancet 1995;345:1609–1610.
8. Zerr I, Pocchiari M, Collins S, et al. Analysis of EEG and CSF 14-3-3 proteins as aids to the diagnosis of Creutzfeldt–Jakob disease. Neurology 2000;55:811–815.
9. Echebarria H, Saiz A, Graus F, et al. Detection of 14-3-3 protein in the CSF of a patient with Hashimoto's encephalopathy. Neurology 2000;54: 1539–1540.
10. Saiz A, Graus F, Dalmau J, et al. Detection of 14-3-3 protein in the cerebrospinal fluid of patients with paraneoplastic neurological disorders. Ann Neurol 1999;46:774–777.
11. Bahn MM, Parchi P. Abnormal diffusion-weighted magnetic resonance images in Creutzfeldt–Jakob disease. Arch Neurol 1999;56:577–583.
12. Zeidler M, Gibbs CJ Jr, Meslin F. WHO manual for strengthening diagnosis and surveillance of Creutzfeldt–Jakob disease. Geneva: World Health Organization, 1998:47–51.
13. Murata T, Shiga Y, Higano S, et al. Conspicuity and evolution of lesions in Creutzfeldt–Jakob disease at diffusion-weighted imaging. AJNR Am J Neuroradiol 2002;23:1164–1172.
14. Fukushima R, Shiga Y, Nakamura M, et al. MRI characteristics of sporadic CJD with valine homozygosity at codon 129 of the prion protein gene and PrPSc type 2 in Japan. J Neurol Neurosurg Psychiatry 2004;75:485–487.
15. Jin K, Shiga Y, Shibuya S, et al. Clinical features of Creutzfeldt–Jakob disease with V180I mutation. Neurology 2004;62:502–505.
16. Inoue I, Kitamoto T, Doh-ura K, et al. Japanese family with Creutzfeldt–Jakob disease with codon 200 point mutation of the prion protein gene. Neurology 1994;44:299–301.
17. Satoh A, Goto H, Satoh H, et al. A case of Creutzfeldt–Jakob disease with a point mutation at codon 232: Correlation of MRI and neurologic findings. Neurology 1997;49:1469–1470.
18. UK Creutzfeldt–Jakob Disease Surveillance Unit. Creutzfeldt–Jakob disease surveillance in the UK eleventh annual report 2002. 2003.
19. Lamstra AW, van Meegen MT, Vreyling JP, et al. 14-3-3 testing in diagnosing Creutzfeldt–Jakob disease. A prospective study in 112 patients. Neurology 2000;55:514–516.
20. Beaudry P, Cohen P, Brandel JP, et al. 14-3-3 protein, neuron-specific enolase, and S-100 protein in cerebrospinal fluid of patients with Creutzfeldt–Jakob disease. Dement Geriatr Cogn Disord 1999;10:40–46.
21. Zeidler M, Will RG, Ironside JW, et al. Magnetic resonance imaging is not a sensitive test for Creutzfeldt–Jakob disease. Br Med J 1996;312:844.
22. Gertz HJ, Henkes H, Cervos-Navvaro J. Creutzfeldt–Jakob disease: correlation of MRI and neuropathologic findings. Neurology 1988;38: 1481–1482.
23. Finkenstaedt M, Szudra A, Zerr I, et al. MR imaging of Creutzfeldt–Jakob disease. Radiology 1996;199:793–798.
24. Schröter A, Zerr I, Henkel H, et al. Magnetic resonance imaging in the clinical diagnosis of Creutzfeldt–Jakob disease. Arch Neurol 2000;57: 1751–1757.
25. McKeith IG, Galasko D, Kosaka K, et al. Consensus guidelines for the clinical and pathologic diagnosis of dementia with Lewy bodies (DLB): Report of the Consortium on DLB International Workshop. Neurology 1996;47:1113–1124.
26. Finelli PF. Diffusion-weighted MR in hypoglycemic coma. Neurology 2001;57:933–935.
27. Arbelaez A, Castillo M, Mukherji SK. Diffusion-weighted MR imaging of global cerebral anoxia. AJNR Am J Neuroradiol 1999;20:999–1007.
28. Mukherjee P, McKinstry RC. Reversible posterior leukoencephalopathy syndrome: evaluation with diffusion-weighted MR imaging. Radiology 2001;219:756–765.
29. Mittal S, Farmer P, Kalina P, et al. Correlation of diffusion-weighted magnetic resonance imaging with neuropathology in Creutzfeldt–Jakob disease. Arch Neurol 2002;59:128–134.
30. Haïk S, Dormont D, Fandeux BA, et al. Prion protein deposits match magnetic resonance imaging signal abnormalities in Creutzfeldt–Jakob disease. Ann Neurol 2002;51:797–799.

Laboratory Investigation (2004) 84, 828–835

www.laboratoryinvestigation.org

Accumulation of prion protein in muscle fibers of experimental chloroquine myopathy: *in vivo* model for deposition of prion protein in non-neuronal tissues

Hisako Furukawa*, Katsumi Doh-ura†, Kensuke Sasaki and Toru Iwaki

Department of Neuropathology, Neurological Institute, Graduate School of Medical Sciences, Kyushu University, Fukuoka, Japan

Prion protein (PrP) is known to accumulate in some non-neuronal tissues under conditions unrelated to prion diseases. The biochemical and biological nature of such accumulated PrP molecules, however, has not been fully evaluated. In this study, we established experimental myopathy in hamsters by long-term administration of chloroquine, and we examined the nature of the PrP molecules that accumulated. PrP accumulation was immunohistochemically demonstrated in autophagic vacuoles in degenerated muscle fibers, and this was accompanied by the accumulation of other molecules related to the neuropathogenesis of prion diseases such as clathrin, cathepsin B, heparan sulfate, and apolipoprotein J. Accumulated PrP molecules were partially insoluble in detergent solution and were slightly less sensitive to proteinase K digestion than normal cellular PrP. Muscle homogenates containing these PrP molecules did not cause disease in inoculated hamsters. The findings indicate that the PrP molecules that accumulated in muscle fibers have distinct biochemical and biological properties. Therefore, experimental chloroquine myopathy is a novel and useful model to investigate the mechanism of deposition of PrP in non-neuronal tissues and might provide new insights in the pathogenesis of prion diseases.
Laboratory Investigation (2004) **84**, 828–835, advance online publication, 3 May 2004; doi:10.1038/labinvest.3700111

Keywords: detergent-solubility; experimental chloroquine myopathy; lysosome; non-neuronal tissues; prion protein; protease sensitivity

Prion diseases such as Creutzfeldt-Jakob disease in humans, and scrapie and bovine spongiform encephalopathy in animals are neurodegenerative disorders characterized by the accumulation in the brain of a protease-resistant, detergent-insoluble abnormal isoform of prion protein (PrP). This abnormal isoform of PrP (PrP^{Sc}) is pathogenic itself and replicates by altering the conformation of a protease-sensitive, detergent-soluble normal cellular isoform of prion protein (PrP^{C}).[1] In addition to the central nervous system, PrP^{Sc} deposition is observed in non-neuronal tissue such as tonsils and skeletal muscles in human prion diseases[2,3] and experimental animals.[4]

PrP is also known to accumulate in non-neuronal tissues under certain pathological conditions unrelated to prion diseases. Frederiske *et al*[5] recently revealed increased PrP immunoreactivity in the regions of fiber-cell degeneration in cataractous lenses in humans. Askanas *et al*[6] reported the accumulation of PrP in vacuolated muscle fibers, in angulated and round atrophic fibers with sarcolemmal enhancement, and in the perivascular inflammatory cells of sporadic inclusion-body myositis in humans.[6,7] It was also reported that the accumulated PrP molecules were sensitive to protease treatment.[7] However, the biochemical and biological characteristics of these PrP molecules have not been fully evaluated.

Chloroquine, a widely used antimalarial agent, is known to be concentrated in lysosomes and to cause elevation of intralysosomal pH.[8] Long-term

Correspondence: Dr H Furukawa, MD, PhD, Department of Pharmacology 1, Nagasaki University Graduate School of Biomedical Sciences, 1-12-4 Sakamoto, Nagasaki 852-8523, Japan.
E-mail: hisako@net.nagasaki-u.ac.jp
*Current address: Department of Pharmacology 1, Nagasaki University Graduate School of Biomedical Sciences, 1-12-4 Sakamoto, Nagasaki 852-8523, Japan.
†Division of Prion Protein Biology, Department of Prion Research, Tohoku University Graduate School of Medicine, 2-1 Seiryo-cho, Aoba-ku, Sendai 980-8575, Japan.
Received 16 January 2004; revised 7 March 2004; accepted 12 March 2004; published online 3 May 2004

administration of chloroquine sometimes causes myopathy, termed chloroquine myopathy (CM), which is characterized by degenerated muscle fibers with numerous autophagic, rimmed vacuoles.[9] Tsuzuki *et al*[10] established experimental CM in the rat to investigate the mechanism of accumulation of the proteins related to Alzheimer's disease in rimmed vacuoles, because of its histopathological similarity to human myopathies where amyloid β deposition is observed in rimmed vacuoles.

To explore the biochemical and biological properties of PrP molecules that accumulate under pathological conditions unrelated to prion diseases, we established experimental CM in hamsters and characterized the PrP molecules (PrP^{CQ}) that accumulated in affected muscle fibers.

Materials and methods

Animals and Reagents

Female Syrian hamsters, 3–8-week old, were purchased from SLC (Hamamatsu, Japan). Chloroquine diphosphate and Nonidet P-40 (NP-40) were purchased from Sigma Chemical (MO, USA). Proteinase K (PK) and complete mini protease inhibitor cocktail were obtained from Roche Molecular Biochemicals (Germany). Monoclonal antibody 3F4 recognizing hamster PrP109-112 was from Senetek (St Louis, MO, USA). Anti-prion protein polyclonal antibody PrP2B was raised by immunization of rabbits with a hamster PrP89-103 fragment. Polyclonal antibodies for apolipoprotein J (clusterin) and for cathepsin B, and monoclonal antibodies CHC5.9 for clathrin and HepSS-1 for heparan sulfate were purchased from Chemicon (Temecula, CA, USA), Calbiochem (Cambridge, MA, USA), PROGEN Biotechnik GmbH (Germany), and Seikagaku Corporation (Japan), respectively.

Experimental CM in Hamsters

Hamsters received 50 mg/kg chloroquine diphosphate (10 mg/ml in sterile saline, pH 7.6) as daily intraperitoneal injections for 60 days. Then the hamsters were killed by decapitation under deep anesthesia. Bilateral soleus, tibialis anterior, and quadriceps muscles were removed and immediately snap-frozen in isopentane cooled with liquid nitrogen. Frozen muscles were kept at −80°C until analysis.

Immunohistochemical Studies

After the blockage of endogenous peroxidase with 0.3% hydrogen peroxide in methanol, serial 10-μm thick sections of frozen muscle were incubated overnight at 4°C with the primary antibodies diluted with 10 mM phosphate-buffered saline (PBS) containing 1% normal hamster serum. The sections were then incubated with horseradish peroxidase-conjugated secondary antibodies for 1 h followed by reactions with 3,3′-diaminobenzidine/H_2O_2 and counterstained with hematoxylin. The serial sections were stained with hematoxylin and eosin (HE), or stained for acid phosphatase or by a modified Gomori-trichrome method.

Brain specimens obtained in some experiments were immersion-fixed in 10% buffered formalin for 24 h at 4°C and embedded in paraffin for immunohistochemical examination. For detection of abnormal PrP deposition, deparaffinized 8-μm thick sections were treated with hydrolytic autoclaving prior to incubation with 3F4 monoclonal antibody.[11]

Protease Sensitivity Assay of PrP^{CQ}

After confirmation of the histological findings, the remaining frozen muscle was homogenized using Tissue-Tearor (Biospec Products, Oklahoma) in 10 volumes of lysis buffer A (0.5% NP-40, 0.5% sodium deoxycholate in PBS pH 7.4). Homogenates were centrifuged at $3300 \times g$ for 15 min to remove the nuclear fraction and debris. The supernatant was then treated with the indicated amount of PK at 37°C for 20 min. After stopping the digestion with 4 mM 4-[2-aminoethyl]-benzenesulfonyl fluoride (Pefabloc, Roche, Germany), an aliquot corresponding to 4 mg of muscle tissue was analyzed by Western blotting using polyclonal antibody PrP2B. Labeled PrP was visualized by using CDP-star detection reagent (Amersham, UK).

Detergent Solubility Assay of PrP^{CQ}

The detergent solubility of PrP^{CQ} was determined as described by Lehmann and Harris[12] with minor modification. Briefly, soleus muscle samples from either control or CM hamsters were homogenized in lysis buffer B (15 mM NaCl, 50 mM Tris-HCl pH 7.5, complete-mini protease inhibitor cocktail) containing the designated concentration of NP-40. Homogenate was centrifuged for 5 min at 1600 *g* to remove debris and the nuclear fraction. The supernatant was ultracentrifuged at 265 000 *g* for 40 min at 25°C. Proteins in the supernatant and in the pellet were separately recovered and analyzed by Western blotting using monoclonal antibody 3F4.

Intracerebral Inoculation of PrP^{CQ}

Inoculum was prepared by homogenizing muscular tissue from CM hamsters or the control in 10 volumes of sterile saline, and 20 μl of the inoculum was injected into the brain of 19 3-week-old female hamsters under deep anesthesia. The hamsters were observed for over 2 years and killed to examine PrP molecules in the brain immunohistochemically.

Densitometry and Statistical Analysis

Blots of the gels were scanned with a CanoScan D2400UF (Canon, Japan). Densities of bands were quantified using NIH Image software. Statistical significance of densitometric data was analyzed by repeated measure ANOVA, and statistical comparison at each dose point between groups was made by Student's *t*-test or Welch's *t*-test.

Ethics

Animal handling and killing were in accordance with the nationally prescribed guidelines, with ethical approval for the study granted by the Animal Experiment Committee of Kyushu University.

Results

Histochemical Findings of CM

All the muscle specimens taken from chloroquine-treated hamsters showed various degrees of myopathic changes accompanied with rimmed vacuoles (Figure 1a), and this was consistent with histopathological findings of experimental CM in the rat.[9,10] In addition to the rimmed vacuoles, many muscle fibers contained coarse granular structures that were strongly stained by hematoxylin (Figure 1c) and modified Gomori trichrome stain (Figure 1g), and they showed enhanced acid phosphatase activity (Figure 1h). These abnormal structures were observed in about 10% of muscle fibers in the soleus muscle which was the most affected in all the muscles of chloroquine-treated hamsters. In contrast, muscles of control hamsters did not contain any rimmed vacuoles or coarse granular structures.

All of the rimmed vacuoles and the coarsely granular structures in degenerated muscle fibers of CM were positively stained by an anti-PrP monoclonal antibody, 3F4, recognizing hamster PrP109-112 (Figure 1b, d). In control hamster muscles, the 3F4 monoclonal antibody reacted with sarcolemmal membranes (data not shown).

To investigate the possible involvement of some molecules that relate to the metabolism of PrP^{C} or the deposition of PrP^{Sc}, serial sections were immunostained for apolipoprotein J (Figure 1e), clathrin (Figure 1f), cathepsin B (Figure 1i), and heparan sulfate (Figure 1j). Immunoreactivities for these molecules were enhanced in the rimmed vacuoles and coarse granular structures in the affected muscle fibers of CM.

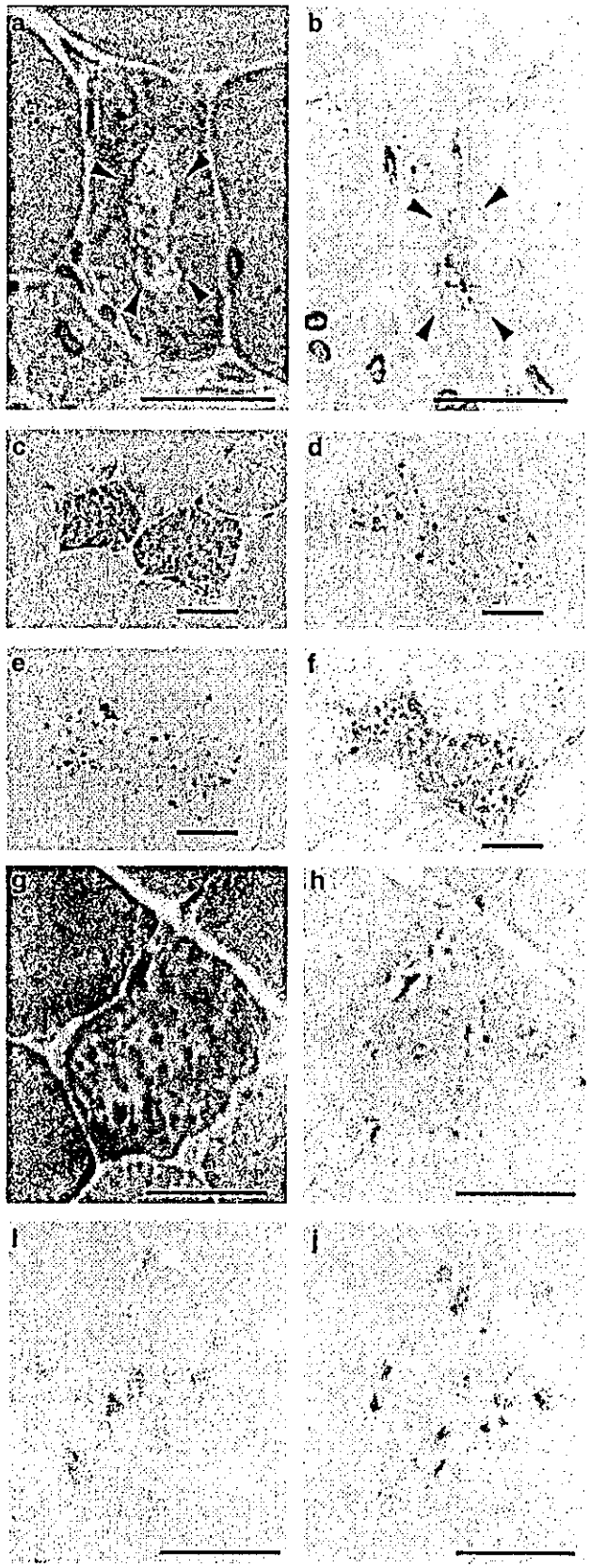

Figure 1 Immunohistochemical findings in CM muscles. Transverse sections of chloroquine-treated (50 mg/kg/day for 60 days) hamster soleus muscles are shown. (a) HE stain shows rimmed vacuole formation (arrow heads). (b) Immunoreactivity for PrP is detected in a rimmed vacuole (arrow heads) shown in (a). (c–f), (g–j) Serial sections stained with HE (c), modified Gomori trichrome (g), acid phosphatase (h), and immunostained for PrP (d), apolipoprotein J (e), clathrin (f), cathepsin B (i), and heparan sulfate (j). Scale bars = 20 μm.

PrP^{CQ} is Slightly Less Sensitive to PK Digestion

Western blot analysis using a polyclonal antibody PrP2B, raised against hamster PrP89-103, revealed prominent bands of 27 and 30 kDa in either CM muscular homogenates or the control, before digestion with PK. There was no significant difference in the intensity of PrP signals between CM muscles and controls (first lanes, Figure 2a, b). The specificity of these bands was confirmed by absorbing the PrP2B antibody with synthetic peptide PrP89-103 (Figure 2c). Although both of the PrP molecules were completely digested with 50 μg/ml of PK, which was the stringent condition to distinguish PrP^{Sc} from PrP^{C} (data not shown), digestion with a smaller amount of PK revealed different PK sensitivity between the PrP molecules from CM muscles (PrP^{CQ}) and PrP^{C} from the control muscles. PrP^{C} derived from control hamster muscle was apparently digested with 0.375 μg/ml of PK, whereas a considerable amount of PrP^{CQ} of 27 kDa still remained after treatment with 1.0 μg/ml of PK (Figure 2a and b). Statistical analysis of the relative density of the bands revealed a significant difference between PrP^{C} and PrP^{CQ} after treatment with 0.5, 0.75, or 1.0 μg/ml of PK (Figure 2d).

PrP^{CQ} is Partially Insoluble in Detergent

Western blot analysis using a monoclonal antibody 3F4 revealed prominent signals at 35 kDa and additional signals at about 30 kDa in the supernatants from either CM muscle homogenate or the control (first lanes, Figure 3a, b). While PrP^{C} from control muscle was completely solubilized in the lysis buffer containing 0.5% NP-40 (Figure 3a), a considerable amount of PrP^{CQ} remained in the

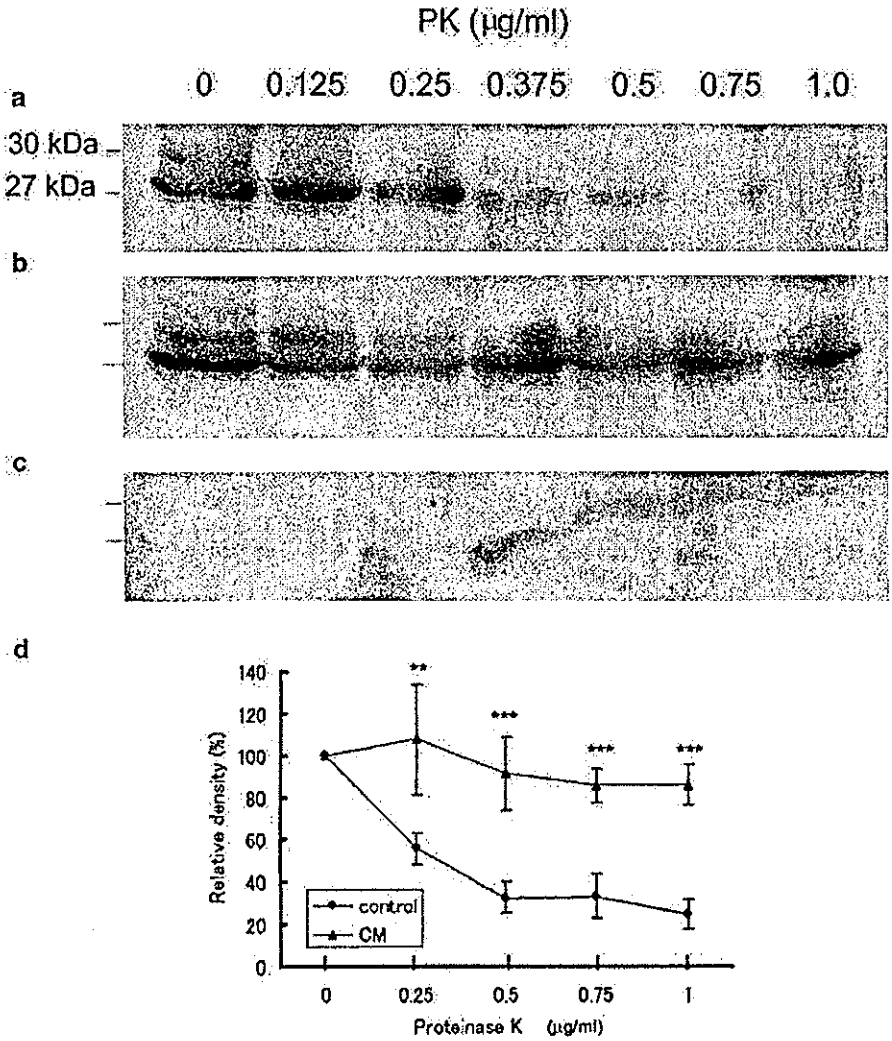

Figure 2 PK sensitivity of PrP molecules in CM muscles. (a–c) PrP molecules in the homogenate of control hamsters (a) or CM hamsters (b) were detected with PrP2B antibody after digestion with a designated amounts of PK at 37°C for 20 min. Prominent bands of 27 kDa and 30 kDa were diminished after the antibody had been absorbed by a synthetic polypeptide used for immunization (c). (d) Densitometric analysis of 27 and 30 kDa bands. Data from three independent experiments are indicated. $^{**}P<0.05$, $^{***}P<0.01$.

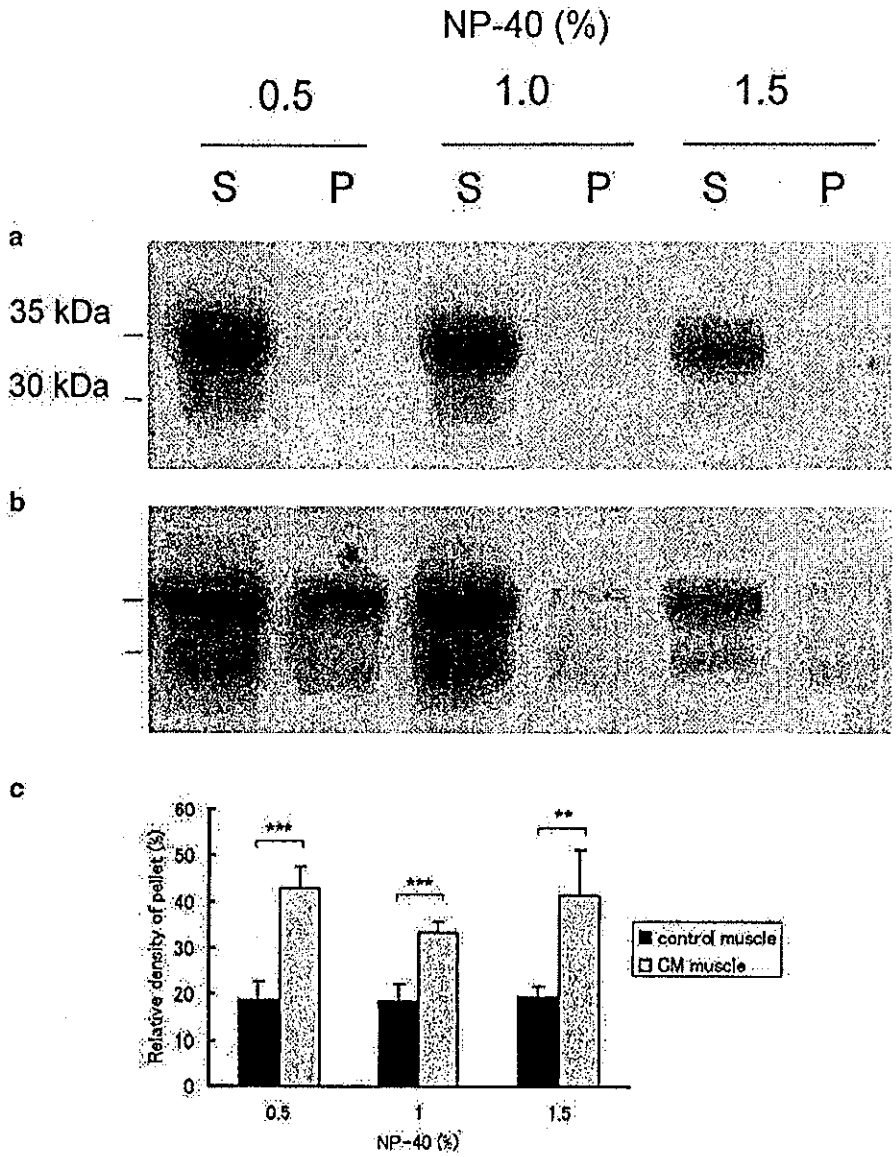

Figure 3 Solubility in NP-40 of PrP molecules in CM muscles. (**a**, **b**) Muscles from control hamsters (a) or CM hamsters (b) were homogenized in the lysis buffer containing designated amount of NP-40 and subsequently ultracentrifuged at 265 000 *g* to separate detergent-soluble PrP molecules in the supernatant (S) and detergent-insoluble molecules in the pellet (P). PrP molecules were labeled with 3F4 monoclonal antibody. (**c**) Relative PrP amount in the pellet fraction. Percentage of PrP signals (30 and 35 kDa) of the pellet fraction in the sum of those of the pellet and the supernatant is shown. Data from three independent experiments. $^{**}P<0.05$, $^{***}P<0.01$.

insoluble fraction in the presence of 0.5, 1.0, or 1.5% NP-40 (Figure 3b, c).

PrP^{CQ} is not Pathogenic

To investigate whether PrP^{CQ} is able to cause pathological changes characteristic of prion diseases *in vivo*, 10% muscular homogenates containing PrP^{CQ} were injected into the brain of Syrian hamsters. The hamsters were observed over 2 years after the inoculation had been given, and none of them developed any signs of prion diseases nor muscle disorders (data not shown). Histological examination of the brain revealed no significant pathological findings or abnormal PrP deposition (Figure 4).

Discussion

In this study, we have demonstrated that slightly less PK-sensitive and partially detergent-insoluble PrP^{CQ} accumulated in affected muscle fibers of experimental CM in hamsters. While PrP molecules from control muscle were sensitive to PK digestion at 0.375 μg/ml and fully soluble in buffer containing 0.5% NP-40, PrP^{CQ} molecules were less sensitive to PK digestion up to 1.0 μg/ml, and a considerable portion of them was insoluble in buffer containing

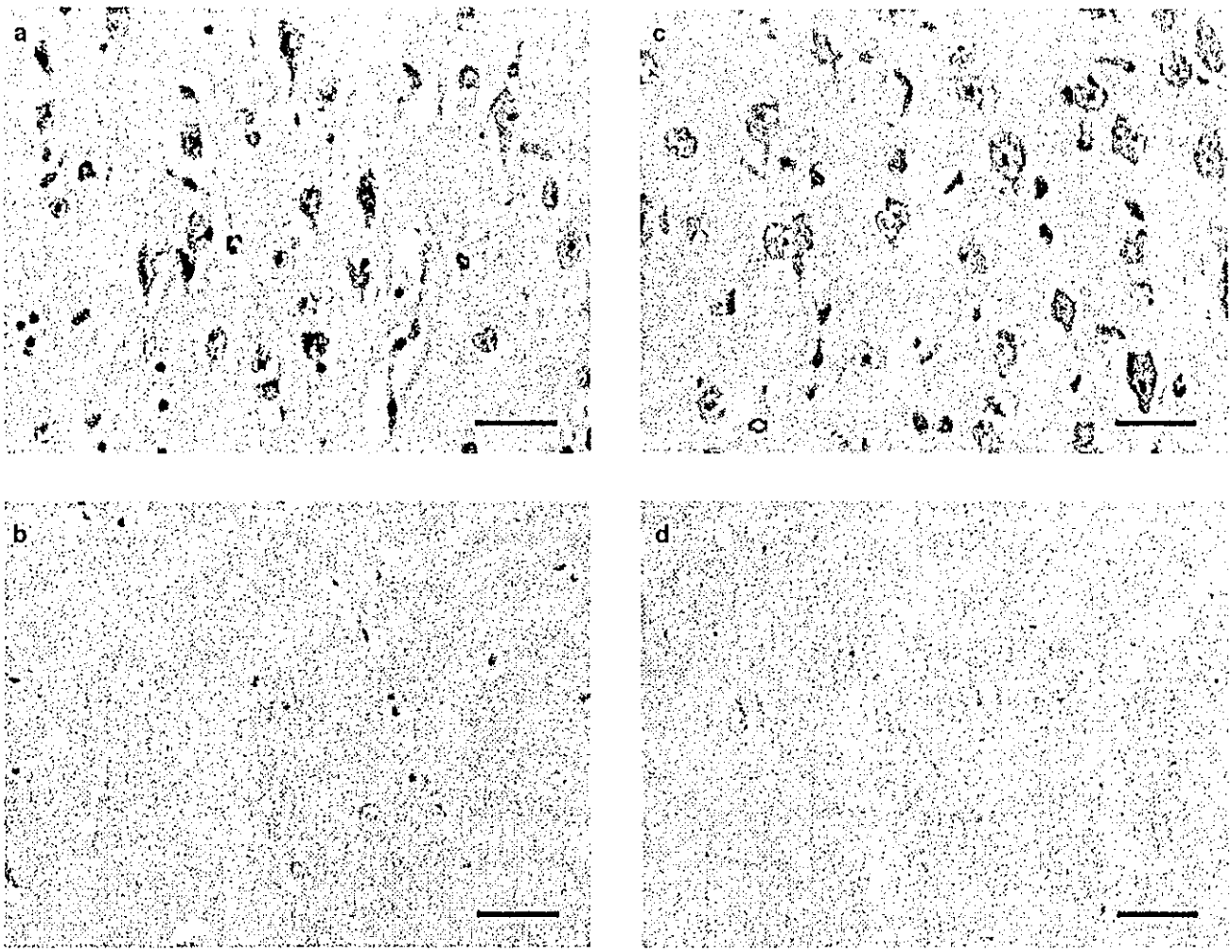

Figure 4 Histological analysis of hamster brain inoculated with CM muscle homogenate. Sections of the brain inoculated with PrP^{C}-containing muscle homogenate (**a**, **b**) or PrP^{CQ}-containing muscle homogenate (**c**, **d**) were stained with HE (**a**, **c**) or immunostained using 3F4 monoclonal antibody (**b**, **d**). Neither neurodegenerative change nor abnormal PrP deposition was revealed. Scale bars = 30 μm.

1.5% NP-40. These biochemical properties of PrP^{CQ} molecules are distinct from PrP^{C}.

There have been several attempts to create *de novo* PrP^{Sc}-like molecules *in vitro*. Using a cell-free conversion system, Horiuchi *et al*[13] were able to convert PrP^{C} into a protease-resistant isoform by the addition of PrP^{Sc} under physiological conditions. Even in the absence of PrP^{Sc}, an acidic buffer can give a β-sheet-dominant conformation and PK resistance to PrP^{C} *in vitro*.[14,15] Nevertheless, no *de novo* PrP^{Sc}-like molecules succeeded to reproduce the disease *in vivo*.[16] In the present study, PrP^{CQ} molecules were not capable of causing any pathological changes in the central nervous system. PrP^{CQ} molecules seem to be distinct from both of these *de novo* PrP^{Sc}-like molecules and PrP^{Sc}, because PrP^{CQ} molecules possess neither marked resistance to PK and detergent insolubility nor transmissibility of the disease conditions.

The CM model reported in this study is different from other PrP-conversion models previously reported, in that PrP^{CQ} molecule was generated *in vivo* in the absence of exogenous input of PrP^{Sc} or PrP^{Sc}-like molecules. Instead, the microenvironment in the lysosome was altered in hamsters by the injection of chloroquine to produce this distinct PrP molecule. Lysosomes are acidic compartments that have been reported to play an important role in the conformational conversion of PrP in prion diseases.[17,18] Chloroquine raises intralysosomal pH to as high as 6.0–6.5, causing marked changes in intracellular protein processing and trafficking.[8] As a consequence of the long-term administration of chloroquine, skeletal muscle fibers degenerate, with numerous autophagic vacuoles.[9] In the process of forming autophagic vacuoles, endogenous muscular PrP^{C} could acquire the properties of PrP^{CQ}.

In the present study, it remains unclear whether chloroquine modifies PrP^{C} molecules directly or indirectly. A previous study revealed that chloroquine does not directly interact with PrP molecules in scrapie-infected neuroblastoma cells.[19]

Furthermore, it has been reported that unfolded recombinant human prion protein PrP90-231 forms a stable protein folding intermediate rich in β-sheet at pH lower than 4.[14] Matsunaga *et al*[20] reported that pH is a crucial factor in determining the conformational state of some amyloidgenic proteins. They found that synthetic Aβ42 and stefin B peptides, showing similar amino-acid alignment to PrP90-144, tend to form amyloid fibrils at acidic pH. Considering these observations, it is unlikely that chloroquine directly interacts with PrP^{C} molecules. An increase in lysosomal pH due to chloroquine, and subsequent metabolic changes in lysosomal systems might be responsible for the biosynthesis of PrP^{CQ} molecules.

Besides experimental CM, there are a few experimental models in which PrP molecules of skeletal muscle are rendered partially PK-resistant and detergent-insoluble. Chiesa *et al*[21] established transgenic mice expressing PrP molecules with nine-octapeptide insertional mutation. Mutated PrP molecules obtained PrP^{Sc}-like properties in the brain and the periphery, producing neurodegeneration similar to an inherited prion disease in humans. In their model, the primary structure of PrP molecules was changed and the mutated PrP was overexpressed not only in the brain but also in the skeletal muscle and heart. This model is quite different from our CM model, in that the primary structure of PrP molecules was not manipulated.

The other experimental model is a transgenic mouse harboring high copy numbers of wild-type PrP transgenes, which spontaneously exhibited necrotizing myopathy, demyelinating polyneuropathy, and focal vacuolation of the central nervous system without apparent deposition of PrP^{Sc}.[22] In spite of severe neurodegeneration and neuromyopathy, only small amount of PK-resistant PrP was detected in affected muscles and brains. They concluded that low level of PK-resistant PrP might reflect aggregation of PrP^{C} and was not correlated with neuropathological changes in these transgenic mice. In our study, PrP^{CQ} after PK digestion did not show molecular characteristics of PrP^{Sc} in prion diseases, suggesting that PrP^{CQ} acquires less PK sensitivity through a different mechanism from that of PrP^{Sc}. Although the expression level of PrP was not increased in CM (data not shown), it is possible that distinct biochemical properties of PrP^{CQ} might simply be due to protein aggregation or alteration in PK–protein ratio, not to the conformational change of monomeric PrP^{C} molecules.

PrP^{CQ} in the affected muscles of the present model was accompanied by the accumulation not only of lysosomal markers but also of those molecules known to be involved in prion disease pathogenesis, such as clathrin, heparan sulfate proteoglycan, and apolipoprotein J.[23–25] It is known that certain sulfated glycans, such as heparan sulfate and pentosan polysulfate, stimulate PrP conversion *in vitro*.[26] Then, it might be possible that accumulated heparan sulfate in the CM muscles contribute to the acquisition of altered PK sensitivity and partial detergent insolubility of the PrP molecules.

Experimental CM in the rat has been established previously as a model of myopathies with rimmed vacuoles, including distal myopathy with rimmed vacuole formation and inclusion-body myositis. Owing to of the deposition of amyloid β in inclusion-body myositis,[27] experimental CM has been utilized by several groups as a peripheral model to investigate the pathogenesis of Alzheimer's disease.[10,28] The precise mechanism of rimmed vacuole formation in CM is still unknown; however, it has been reported that chloroquine causes an increase in endogenous autophagosomes in mammalian cells.[29] Similar mechanism(s) might be shared between amyloid β deposition in the CM rat model and PrP^{CQ} accumulation in our CM hamster model.

The PrP2B polyclonal antibody revealed prominent 27 kDa signals with additional 30 kDa signals (Figure 2), while the 3F4 monoclonal antibody reacted with dominant 35 kDa signals and additional 30 kDa signals (Figure 3), which were similar to Cp33-37 signal in skeletal muscle of hamster.[30] The common signals of 30 kDa were detected by both of the two antibodies. Minor epitope differences between the two antibodies might account for such a diversity of PrP signals, but it remains to be elucidated.

Finally, together with the biochemical and biological properties of PrP^{CQ}, the immunohistochemical findings in CM muscles of the molecules known to be involved in prion disease pathogenesis indicate that experimental CM in hamsters is a useful *in vivo* model to investigate the mechanism of PrP accumulation in the pathogenesis of PrP-related diseases.

Acknowledgements

We are grateful to Professor Mitsuo Takahashi at Fukuoka University and Professor Masami Niwa at Nagasaki University for their critique and suggestions on the research and this report. The English used in this manuscript was revised by Universal Academy Press, Inc., Japan.

This work was supported by a grant (H13-kokoro-025) to KD from the Ministry of Health, Labor and Welfare of Japan.

References

1 Prusiner SB. Molecular biology of prion diseases. Science 1991;252:1515–1522.
2 Hill AF, Zeidler M, Ironside J, *et al.* Diagnosis of new variant Creutzfeldt-Jakob disease by tonsil biopsy. Lancet 1997;349:99–100.
3 Glazel M, Abela E, Maisson M, *et al.* Extraneural pathologic prion protein in sporadic Creutzfeldt–Jakob disease. N Eng J Med 2003;349:1812–1820.

4 Bosque PJ, Ryou C, Telling G, *et al.* Prions in skeletal muscle. Proc Natl Acad Sci USA 2002;99:3812–3817.
5 Frederikse PH, Zigler Jr SJ, Farnsworth PN, *et al.* Prion protein expression in mammalian lenses. Curr Eye Res 2000;20:137–143.
6 Askanas V, Bilak M, Engel WK, *et al.* Prion protein is abnormally accumulated in inclusion-body myositis. Neuroreport 1993;5:25–28.
7 Zanusso G, Vattemi G, Ferrari S, *et al.* Increased expression of the normal cellular isoform of prion protein in inclusion-body myositis, inflammatory myopathies and denervation atrophy. Brain Pathol 2001;11:182–189.
8 Holzman E. Lysosomes. Cellular organelles. Plenum Press: New York and London, 1989.
9 Macdonald RD, Engel AG. Experimental chloroquine myopathy. J Neuropath Exp Neurol 1970;29:479–499.
10 Tsuzuki K, Fukatsu R, Takamaru Y, *et al.* Co-localization of amyloid-associated proteins with amyloid beta in rat soleus muscle in chloroquine-induced myopathy: a possible model for amyloid beta formation in Alzheimer's disease. Brain Res 1995;699:260–265.
11 Kitamoto T, Shin RW, Doh-ura K, *et al.* Abnormal isoform of prion protein accumulates in the synaptic structures of the central nervous system in patients with Creutzfeldt–Jakob disease. Am J Path 1992;140: 1285–1294.
12 Lehmann S, Harris DA. Blockade of glycosylation promotes acquisition of scrapie-like properties by the prion protein in cultured cells. J Biol Chem 1997; 272:21479–21487.
13 Horiuchi M, Caughey B. Specific binding of normal prion protein to the scrapie form via a localized domain initiates its conversion to the protease-resistant state. EMBO J 1999;18:3193–3203.
14 Swietnicki W, Peterson R, Gambetti P, *et al.* pH-dependent stability and conformation of the recombinant human prion protein PrP(90-231). J Biol Chem 1997;272:27517–27520.
15 Matsunaga Y, Peretz D, Williamson A, *et al.* Cryptic epitope in N-teminally truncated prion protein are exposed in the full-length molecule: dependence of conformation on pH. Proteins 2001;44:110–118.
16 Hill AF, Antoniou M, Collinge J. Protease-resistant prion protein produced *in vitro* lacks detectable infectivity. J Gen Virol 1999;80:11–14.
17 Laszlo L, Lowe J, Self T, *et al.* Lysosomes as key organelles in the pathogenesis of prion encephalopathies. J Pathol 1992;166:333–341.
18 Shyng SL, Huber MT, Harris DA. A prion protein cycles between the cell surface and an endocytic compartment in cultured neuroblastoma cells. J Biol Chem 1993;268:15922–15928.
19 Doh-ura K, Iwaki T, Caughey B. Lysosomotropic agents and cysteine protease inhibitors inhibit scrapie-associated prion protein accumulation. J Virol 2000;74:4894–4897.
20 Matsunaga Y, Zerovnik E, Yamada T, *et al.* Conformational changes preceding amyloid-fibril formation of amyloid-beta and stefin B: parallels in pH dependence. Curr Med Chem 2002;9:1717–1724.
21 Chiesa R, Pestronk A, Schmidt RE, *et al.* Primary myopathy and accumulation of PrPSc-like molecules in peripheral tissues of transgenic mice expressing a prion protein insertional mutation. Neurobiol Dis 2001;8:279–288.
22 Westaway D, DeArmond SJ, Cayetano-Canlas J, *et al.* Degeneration of skeletal muscle, peripheral nerves, and the central nervous system in transgenic mice overexpressing wild-type prion proteins. Cell 1994; 76:117–129.
23 Mouillet-Richard S, Ermonval M, Chebassier C, *et al.* Signal transduction through prion protein. Science 2000;289:1925–1928.
24 McBride PA, Wilson MI, Eikeleboom P, *et al.* Heparan sulfate proteoglycan is associated with amyloid plaques and neuroanatomically targeted PrP pathology throughout the incubation period of scrapie-infected mice. Exp Neurol 1998;149:447–454.
25 Sasaki K, Doh-ura K, Ironside JW, *et al.* Increased clusterin (apolipoprotein J) expression in human and mouse brains infected with transmissible spongiform encephalopathies. Acta Neuropathol (Berl) 2002;103: 199–208.
26 Wong C, Xiong LW, Horiuchi M, *et al.* Sulfated glycans and elevated temperature stimulate PrP^{Sc}-dependent cell-free formation of protease-resistant prion protein. EMBO J 2001;20:377–386.
27 Askanas V, Engel WK, Alvarez RB, *et al.* Beta-amyloid protein immunoreactivity in muscle of patients with inclusion-body myositis. Lancet 1992; 339:560–561.
28 Murakami N, Oyama F, Gu Y, *et al.* Accumulation of tau in autophagic vacuoles in chloroquine myopathy. J Neuropathol Exp Neurol 1998;57:664–673.
29 Suzuki T, Nakagawa M, Yoshikawa A, *et al.* The first molecular evidence that autophagy relates rimmed vacuole formation in chloroquine myopathy. J Biochem 2002;131:647–651.
30 Bendheim PE, Brown HR, Rudelli RD, *et al.* Nearly ubiquitous tissue distribution of the scrapie agent precursor protein. Neurology 1992;42:149–156.

JOURNAL OF VIROLOGY, May 2004, p. 4999–5006 Vol. 78, No. 10
0022-538X/04/$08.00+0 DOI: 10.1128/JVI.78.10.4999–5006.2004

Treatment of Transmissible Spongiform Encephalopathy by Intraventricular Drug Infusion in Animal Models

Katsumi Doh-ura,[1]* Kensuke Ishikawa,[1]† Ikuko Murakami-Kubo,[1] Kensuke Sasaki,[1] Shirou Mohri,[2] Richard Race,[3] and Toru Iwaki[1]

Department of Neuropathology[1] and Center of Biomedical Research,[2] Graduate School of Medical Sciences, Kyushu University, Fukuoka 812-8582, Japan, and Laboratory of Persistent Viral Diseases, Rocky Mountain Laboratories, National Institute of Allergy and Infectious Diseases, National Institutes of Health, Hamilton, Montana 59840[3]

Received 6 October 2003/Accepted 9 January 2004

The therapeutic efficacy of direct drug infusion into the brain, the target organ of transmissible spongiform encephalopathies, was assessed in transgenic mice intracerebrally infected with 263K scrapie agent. Pentosan polysulfate (PPS) gave the most dramatic prolongation of the incubation period, and amphotericin B had intermediate effects, but antimalarial drugs such as quinacrine gave no significant prolongation. Treatment with the highest dose of PPS at an early or late stage of the infection prolonged the incubation time by 2.4 or 1.7 times that of the control mice, respectively. PPS infusion decreased not only abnormal prion protein deposition but also neurodegenerative changes and infectivity. These alterations were observed within the brain hemisphere fitted with an intraventricular infusion cannula but not within the contralateral hemisphere, even at the terminal disease stage long after the infusion had ended. Therapeutic effects of PPS were also demonstrated in mice infected with either RML agent or Fukuoka-1 agent. However, at doses higher than that providing the maximal effects, intraventricular PPS infusion caused adverse effects such as hematoma formation in the experimental animals. These findings indicate that intraventricular PPS infusion might be useful for the treatment of transmissible spongiform encephalopathies in humans, providing that the therapeutic dosage is carefully evaluated.

Transmissible spongiform encephalopathies (TSEs), or prion diseases, are fatal neurodegenerative disorders that include Creuzfeldt-Jakob disease (CJD) and Gerstmann-Sträussler-Scheinker disease in humans, in addition to scrapie and bovine spongiform encephalopathy in animals. These disorders are characterized by deposition in the brain of a protease-resistant isoform of prion protein (PrP), which is thought to be the main pathogenic component responsible for the pathogenesis (18). Outbreaks of acquired forms of human TSEs, such as variant CJD (21) and iatrogenic CJD with cadaveric growth hormone or dura grafts (3) in younger people, are prompting the development of prophylactic and therapeutic interventions.

There are some chemicals that are effective in inhibiting the accumulation or conformational change of PrP molecules in vitro and/or in prolonging the incubation period when they are administered around the time of infection in TSE animal models (2, 17). However, no chemicals, except for amphotericin B and one of its derivatives, have been reported to improve prognosis when they are administered late in the disease course or after the infectious agent has already invaded the brain (8). This implies that it may be difficult to improve the prognosis in human patients by using chemicals, because patients first come to medical attention after the onset of neurological symptoms.

Most of the previously reported chemicals have been large and hydrophilic, and whether their ineffectiveness was actually due to their poor accessibility to the brain has not been evaluated. We have developed a more sensitive drug evaluation system, which does not depend on drug accessibility to the brain, by implanting a continuous intraventricular drug infusion device into an intracerebrally TSE-infected animal model. Using this model, we have examined clinically applicable chemicals that have previously been reported to be effective either in vitro or in vivo, including antimalarial drugs such as quinacrine and chloroquine, the E-64d cysteine protease inhibitor, amphotericin B, and pentosan polysulfate (PPS). We report that intraventricular administration of PPS through the infusion device inhibited not only abnormal PrP accumulation but also neurodegenerative changes and infectivity in the brain, thereby giving rise to a dramatic prolongation of the life spans of intracerebrally infected animals.

MATERIALS AND METHODS

Experimental animals and in vivo evaluation. Tg7 mice, which are derived from Tg10 mice (19) and express hamster PrP but not endogenous mouse PrP, were inoculated with 20 μl of 1% 263K agent hamster homogenate in the right parietal portion of the brain. An Alzet osmotic pump (Durect, Cupertino, Calif.) filled with a chemical was placed in a subcutaneous area of the back. An intraventricular infusion cannula connected to the osmotic pump through a catheter was implanted in the left frontal portion of the brain in order to place the cannula tip into the left ventricle at either day 10 or 35 postinoculation or at another designated time. The pump worked stably from 40 h after implantation and continuously for 4 weeks. Five to 10 male mice per group, each weighing about 35 g, were used. Each mouse was kept in an individual cage under the same feeding and watering conditions in an air-conditioned, light time-controlled, specific-pathogen-free room. The mice began to exhibit ambiguous signs of reduced activity about 2 days prior to death, followed by obvious signs of ruffled

* Corresponding author. Present address: Department of Prion Research, Tohoku University Graduate School of Medicine, 2-1 Seiryo-cho, Aoba-ku, Sendai 980-8575, Japan. Phone: 81-22-717-8232. Fax: 81-22-717-8148. E-mail: doh-ura@mail.tains.tohoku.ac.jp.

† Present address: Department of Prion Research, Tohoku University Graduate School of Medicine, Sendai 980-8575, Japan.

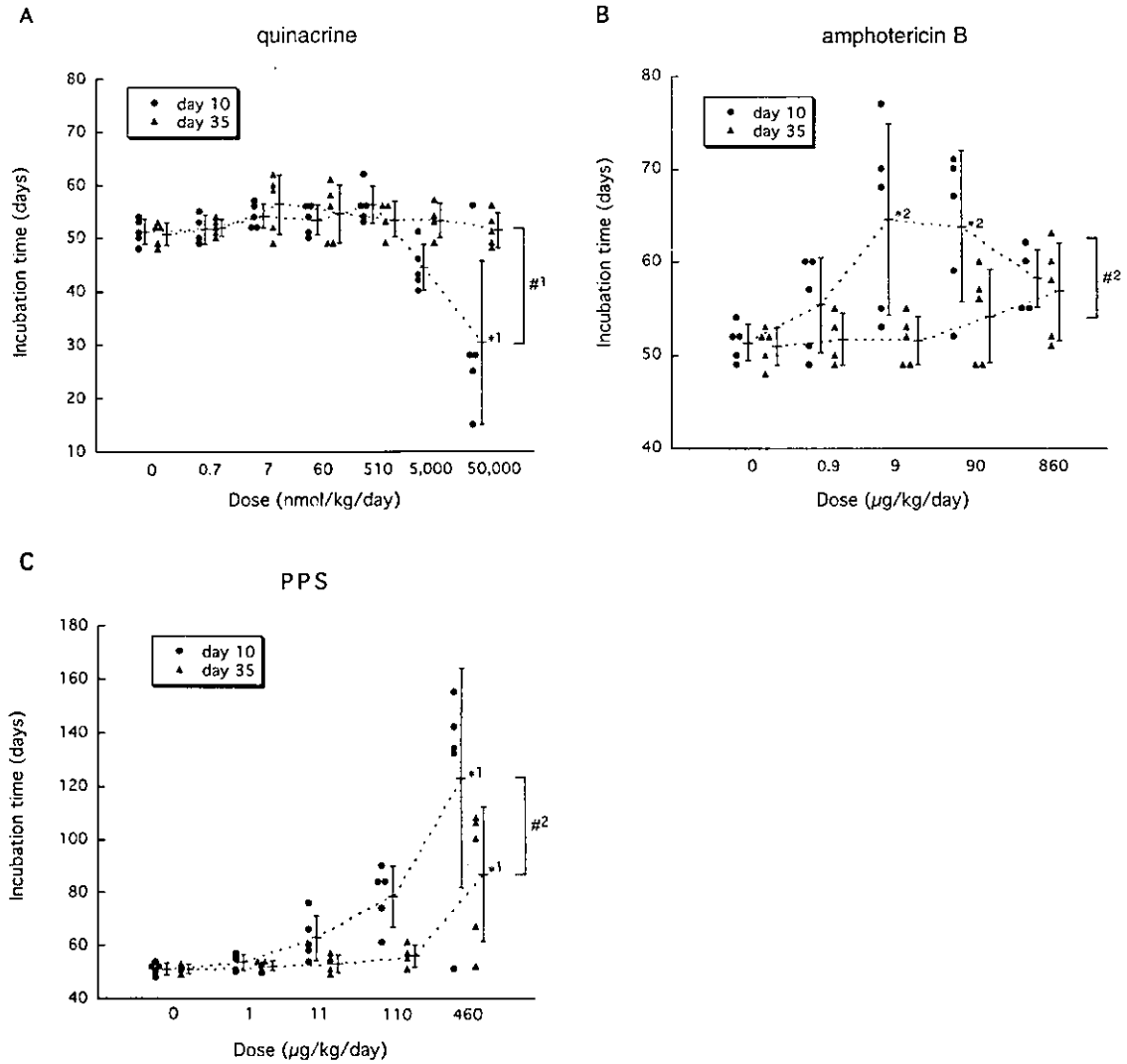

FIG. 1. Efficacy of quinacrine (A), amphotericin B (B), and PPS (C) in intracerebrally infected mice. Intraventricular infusion of a chemical was initiated at an early infection stage (day 10 postinoculation) or at a late stage (day 35) in 263K-infected Tg7 mice and continued for 4 weeks. Each circle or triangle represents an individual mouse. Bars represent the means and standard deviations of the incubation times for each group. *1, $P < 0.05$ versus the neighboring group and $P < 0.01$ versus the other groups; *2, $P < 0.05$ versus the vehicle control; #1, $P < 0.05$, #2, $P < 0.01$.

fur and bradykinesia on the day before or the day of death. The incubation period during which the animals were observed every day lasted from the time of intracerebral infection to the time of an obvious clinical stage.

Tga20 mice (14), which overexpress mouse PrP, were similarly inoculated with 1% RML agent mouse homogenate or 1% Fukuoka-1 agent mouse homogenate, and 4-week continuous intraventricular infusion of a chemical was started at day 14 or 49 postinoculation as described above.

Chemicals. The E-64d cysteine protease inhibitor was generously provided by S. Ishiura, Tokyo University, Tokyo, Japan. Quinacrine and chloroquine were obtained from Sigma. Amphotericin B (Fungizone) was purchased from Bristol-Myers Squibb (Tokyo, Japan). The sodium salt of PPS (Cartrophen Vet) was purchased from Biopharm (Bondi Junction, New South Wales, Australia) and used after removal of an alcohol additive by drying. E-64d was dissolved in dimethyl sulfoxide, amphotericin B was dissolved in distilled water, and all other chemicals were dissolved in phosphate-buffered saline (PBS).

Immunohistochemistry, immunoblotting, and infectivity assay. Mouse brains were fixed with 10% formalin and embedded in paraffin. Sections (5 μm thick) of the coronal slice sited around one-third of the distance from the interaural line to the bregma line were dewaxed and immunostained with an anti-PrP-C antibody (1:200; Immuno-Biological Labs, Gunma, Japan) or an antibody against glial fibrillary acidic protein (GFAP) (1:1,000; Dako, Glostrup, Denmark) as previously described (11).

For the detection of protease-resistant PrP (PrPres) by immunoblotting, the whole brain hemisphere where the intraventricular cannula had been fitted was homogenized with a ninefold volume of lysis buffer (0.5% sodium deoxycholate, 0.5% Nonidet P-40, PBS), and following low-speed centrifugation, the supernatant (Sup1) was treated with 25 μg of proteinase K per ml for 30 min at 37°C. An aliquot corresponding to 2.0 mg of brain tissue was electrophoresed in a sodium dodecyl sulfate–15% polyacrylamide gel and electroblotted onto a polyvinylidene difluoride filter. The filter was incubated with an anti-PrP-2B antibody raised against a hamster PrP fragment (amino acids 89 to 103) and then with an alkaline phosphatase-conjugated secondary antibody (Promega). Signals were visualized with CDP-Star detection reagent (Amersham).

For the infectivity assay, an aliquot of the Sup1 described above was diluted with PBS to produce a 0.1% brain homogenate, and a 20-μl aliquot of this homogenate was then inoculated intracerebrally in Tg7 mice. The infectious titer was calculated from the incubation period based on standard data obtained from an inoculation study with serially diluted homogenate samples of 263K-infected, terminally diseased brain tissue.

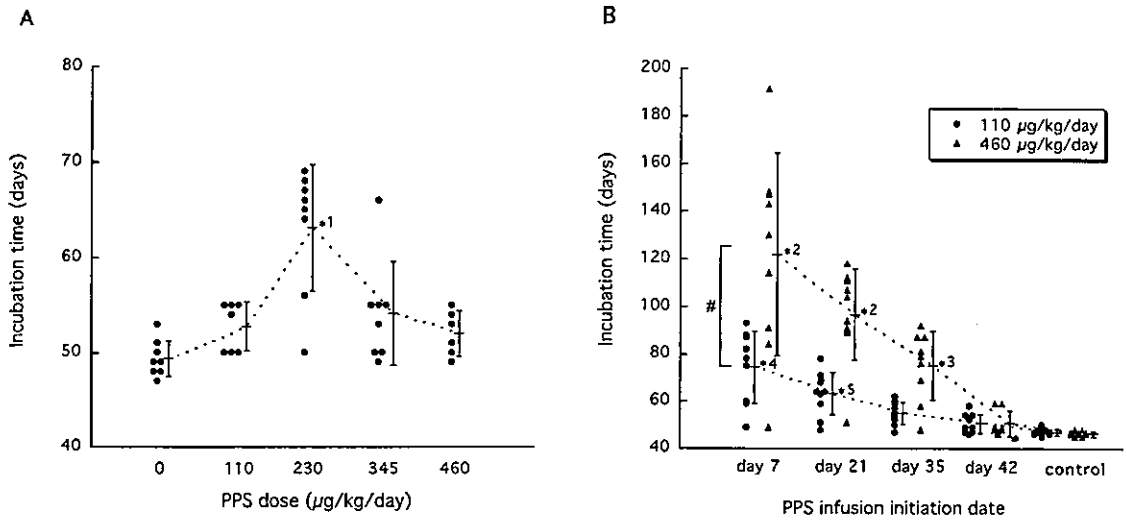

FIG. 2. Dose response (A) and administration timing (B) in PPS efficacy. Intraventricular infusion at the indicated concentrations (A) or at 110 or 460 μg/kg/day (B) was initiated at day 42 postinoculation (A) or at the indicated times (B) in intracerebrally 263K-infected Tg7 mice. *1, $P < 0.01$ versus the other groups; *2, $P < 0.01$ versus the other groups except the neighboring group(s); *3, $P < 0.05$ versus the control; *4, $P < 0.05$ versus the neighboring group and $P < 0.01$ versus the other groups; *5, $P < 0.01$ versus the control; #, $P < 0.01$.

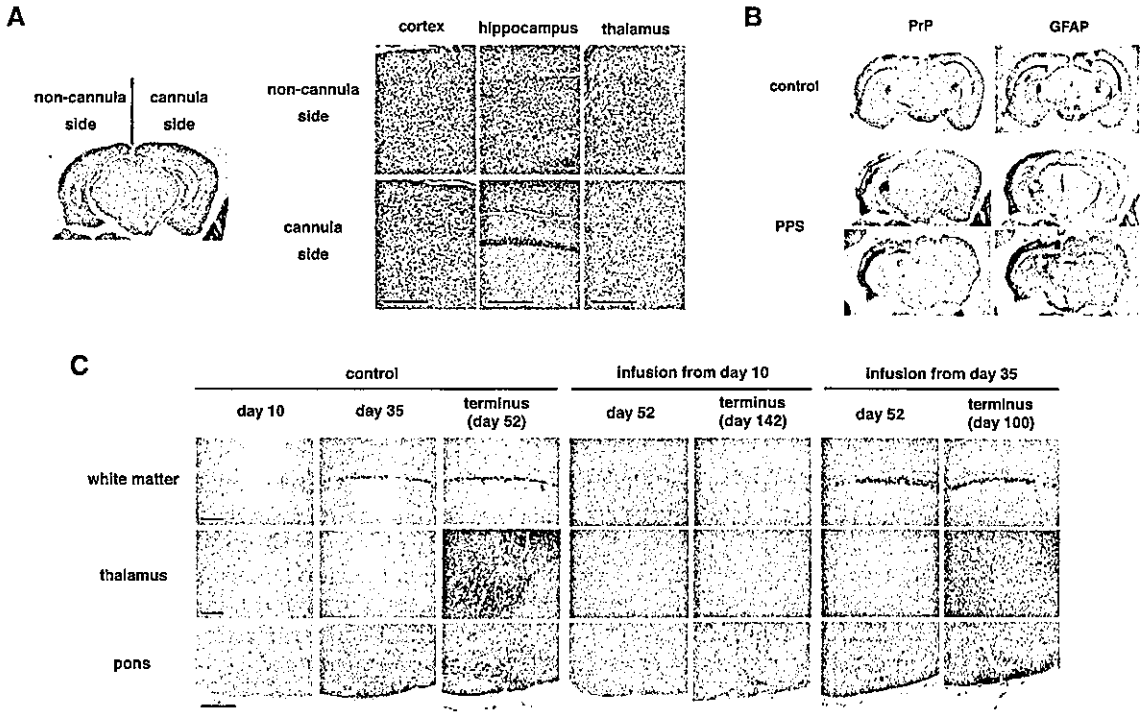

FIG. 3. Histopathology of the brain with or without PPS treatment. (A) Histology of the brain from an intracerebrally 263K-infected, long-surviving mouse treated with PPS at 460 μg/kg/day from day 10 postinoculation. Noncannula side and cannula side represent the sides of pathogen inoculation and intraventricular cannula implantation, respectively. Hematoxylin-eosin staining was used. (B) Immunohistochemical detection of abnormal PrP deposition (PrP) and of neurodegenerative changes by means of glial reaction (GFAP) in the same brain as for panel A (PPS) or in the brain from a nontreated mouse (control). The orientation of the sides of pathogen inoculation and cannula implantation is the same as in panel A. A coronal section sited around one-third of the distance from the interaural line to the bregma line is shown for the control mouse, and either a coronal section sited around one-third of the distance or a coronal section sited around two-thirds of the distance from the interaural line to the bregma line is shown for the PPS-treated mouse. Astrocytic glial reaction is demonstrated by immunohistochemistry for GFAP. (C) Sequential analysis of abnormal PrP deposition in intracerebrally 263K-infected, nontreated mice (control) or mice treated with PPS (infusion from day 10 or 35). Each panel shows a representative finding from three mice sacrificed at a designated time. In PPS-treated mice, the brain tissue examined was obtained from the hemisphere implanted with the intraventricular cannula, which was the hemisphere opposite to that of the inoculation site. PPS was infused at 460 μg/kg/day from day 10 or 35 postinoculation. Each image of the hippocampus or the thalamus (posterior nuclei) is from coronal sections sited around one-third of the distance from the interaural line to the bregma line. Each image of the pons (ventral area) is from a coronal section which is parallel to the interaural line and contains the culmen portion of the cerebellum. Bar, 160 μm.